

## Supplementary Information

Conor Jason Price\* and Steven Paul Hepplestone†

*Department of Physics, University of Exeter,  
Stocker Road, Exeter, EX4 4QL, United Kingdom*

**CONTENTS**

I. Methodology	S3
A. Calculation Details	S3
B. k-Point Testing	S6
1. Graphite Results	S6
2. Lithium Cobalt Oxide Results	S9
C. Summary of Previous Work	S12
1. Comparison of T-Phase and H-Phase TMDCs	S12
2. Intercalation Stability	S13
II. Results	S16
A. Single Crystal Bulk Modulus	S16
B. Elastic Tensors	S20
1. Materials Project	S30
C. Elastic Stability	S32
D. Elastic Quantities	S34
E. Material Anisotropy	S47
1. Universal Anisotropy and Elastic Constants	S47
2. Anisotropic Young's Modulus	S52
References	S54

## I. METHODOLOGY

### A. Calculation Details

In Table SI, the valence electrons considered for each species are presented. The projector augmented wave method<sup>1</sup> was used to describe the interaction between core and valence electrons, and a plane-wave basis set was used with an energy cutoff of 700 eV. All structural relaxations were completed using the Perdew-Burke-Ernzerhof (PBE) functional<sup>2</sup> using the conjugate gradient algorithm and converged to a force tolerance of 0.0001 eV/Å per atom, and electronic self-consistency is considered to an accuracy of  $10^{-7}$  eV. Elastic properties were obtained using Monkhorst-Pack grids<sup>3</sup> of  $k$ -points equivalent to a  $18 \times 18 \times 18$  grid in the primitive cells. The PBE<sup>2</sup> functional form of the generalised gradient approximation (GGA) was used with the van der Waals interactions addressed using the zero damping DFT-D3 method of Grimme<sup>4</sup>. For evaluation of the elastic matrix symmetry, elements are considered to be equal if they fall within 0.01 GPa.

Many works have shown that choice of functional can lead to differences in predictions for properties important to electrode materials<sup>5,6</sup>. Previous works have found that use of hybrid functionals such as HSE06 demonstrate a change of  $\sim 5\%$  in the matrix elements and elastic values in monolayers of CaFI<sup>7</sup> and CaFCl<sup>8</sup> compared to GGA method, and a change of  $\sim 10\%$  for BiAlO<sub>3</sub><sup>9</sup>. Compared to GGA functionals, +U corrections have been shown to reduce the elements of the elastic tensor and produce small deviations in some elastic properties for CuInTe<sub>2</sub><sup>10</sup>, and increase elastic constants in FePO<sub>4</sub><sup>11</sup> resulting in an increase in the bulk and shear moduli. +U has also been shown to produce little change to the values obtained for LiFePO<sub>4</sub><sup>11</sup>. The functionals rVV10 and VdW-DF2 have produced similar values to the PBE functional<sup>12</sup> for bulk and monolayer MoS<sub>2</sub>, with no significant improvement to the matrix elements or elastic constants compared to the values obtained using experimental methods.

Computational studies<sup>13,14</sup> on 2H-MoS<sub>2</sub> have also been used to compare results obtained with different levels of exchange-correlation approximation to those obtained experimentally. For example, the  $c_{11}$  element is found to have an experimental value of 238 GPa which is reproduced with HSE methods, but underestimated at 211 GPa using a GGA functional. However, other elements of the elastic matrix are more accurately calculated using GGA

than with HSE, though these typically fall within  $\sim 10\%$  of experiment. There is also a spread in values for any given method (for example, between different calculations using GGA), suggesting that other aspects of a first principles calculation offer more significant changes to elastic results than the level of exchange-correlation approximation employed. Finally, we have also performed a limited study on the elastic properties of graphite and LiCoO<sub>2</sub> using the PBE functional. This is outlined in Section S1B, where we find close agreement with experimental results, improving on LDA and other GGA results in the case of graphite, and improving on LDA, other GGA, and HSE results in the case of LiCoO<sub>2</sub>.

In this work we have chosen to use the PBE functional for three reasons: (i) the increased computational cost of using hybrid functionals; (ii) the lack of experimental results for many of the materials considered necessary for accurate choice of +U corrections, and (iii) the relatively small changes to the elastic properties that arise from these methods.

Given the possible complexity of magnetic ordering in TMDCs, there can be many local minima in the potential energy surface, and the global minimum might not be easily identifiable. This ambiguity increases the risk of drawing incorrect conclusions from spin-orbit (SO) calculations. Further, despite the additional cost and time, calculations including SO may not yield significantly distinct properties compared to simpler calculations. In the case of the TMDCs, numerous prior studies have already examined the influence of spin-orbit effects on their electronic structure. Typically, the spin-orbit interaction can be thought of as a modulation on the electronic structure. Specifically for elastic properties, some previous works have compared results of transition-metal containing compounds obtained with and without the SO interaction. Small ( $\sim 1\%$ ) change in  $c_{11}$  and  $c_{12}$  when doping Ni<sub>24</sub>Al<sub>7</sub> with transition metals, and the effect is a lot less significant compared to that arising from the inclusion of spin<sup>15</sup>. There is also a small ( $\sim 5\%$ ) change in the in-plane elastic constants of monolayers of HfSSe, and no change in the HfS<sub>2</sub> and HfSe<sub>2</sub> equivalents<sup>16</sup>. One material composed of Period V and VI elements, YPtBi, shows an increase in  $c_{11}$ ,  $c_{12}$  and  $c_{44}$  by  $\sim 10\%$  with the inclusion of SO<sup>17</sup>. However, we consider this change to be at the extreme end due to the high content of heavy elements compared to the TMDCs considered in this work.

Species	Included Electrons	Species	Included Electrons
Li	1s <sup>2</sup> 2s <sup>1</sup> (3)	Re	5d <sup>6</sup> 6s <sup>1</sup> (7)
Mg	2p <sup>6</sup> 3s <sup>2</sup> (8)	Fe	3d <sup>7</sup> 4s <sup>1</sup> (8)
S	3s <sup>2</sup> 3p <sup>4</sup> (6)	Ru	4s <sup>2</sup> 4p <sup>6</sup> 4d <sup>7</sup> 5s <sup>1</sup> (16)
Se	4s <sup>2</sup> 4p <sup>4</sup> (6)	Os	5d <sup>7</sup> 6s <sup>1</sup> (8)
Te	5s <sup>2</sup> 5p <sup>4</sup> (6)	Co	3d <sup>8</sup> 4s <sup>1</sup> (9)
Sc	3d <sup>2</sup> 4s <sup>1</sup> (3)	Rh	4d <sup>8</sup> 5s <sup>1</sup> (9)
Y	4s <sup>2</sup> 4p <sup>6</sup> 4d <sup>2</sup> (10)	Ir	5d <sup>8</sup> 6s <sup>1</sup> (9)
Ti	3p <sup>6</sup> 3d <sup>3</sup> 4s <sup>1</sup> (10)	Ni	3d <sup>9</sup> 4s <sup>1</sup> (10)
Zr	4s <sup>2</sup> 4p <sup>6</sup> 4d <sup>3</sup> (11)	Pd	4d <sup>9</sup> 5s <sup>1</sup> (10)
Hf	5d <sup>3</sup> 6s <sup>1</sup> (4)	Pt	5d <sup>9</sup> 6s <sup>1</sup> (10)
V	3d <sup>4</sup> 4s <sup>1</sup> (5)	Cu	3d <sup>10</sup> 4s <sup>1</sup> (11)
Nb	4s <sup>2</sup> 4p <sup>6</sup> 4d <sup>4</sup> 5s <sup>1</sup> (13)	Ag	4d <sup>10</sup> 5s <sup>1</sup> (11)
Ta	5d <sup>4</sup> 6s <sup>1</sup> (5)	Au	5d <sup>10</sup> 6s <sup>1</sup> (11)
Cr	3s <sup>2</sup> 4s <sup>1</sup> 4p <sup>6</sup> 4d <sup>5</sup> (14)	Ge	3d <sup>10</sup> 4s <sup>2</sup> 4p <sup>2</sup> (14)
Mo	4d <sup>5</sup> 5s <sup>1</sup> (6)	Sn	4d <sup>10</sup> 5s <sup>2</sup> 5p <sup>2</sup> (14)
W	5d <sup>5</sup> 6s <sup>1</sup> (6)	Pb	5d <sup>10</sup> 6s <sup>2</sup> 6p <sup>2</sup> (14)
Mn	3p <sup>6</sup> 3d <sup>6</sup> 4s <sup>1</sup> (13)		

Table S I: Electronic configurations of electrons modelled for different species considered in this study.

## B. k-Point Testing

Due to the small changes in energy that can be involved, the elements of the elastic tensor can be sensitive to the sampling of reciprocal space<sup>18</sup>. For the primitive unit cells considered, Monkhorst-Pack k-point grids of  $18 \times 18 \times 18$  were used, and for the  $2 \times 2 \times 2$  supercells comparable grids of  $9 \times 9 \times 9$ . These correspond to k-point densities of 17,496 per reciprocal atom (pra) in the pristine systems, and 23,328 pra in the intercalated systems. These values are comparable to those used in databases such as the Materials Project<sup>19,20</sup>, and in similar studies of other layered materials<sup>21–25</sup>.

The limited number of studies into the elastic properties of the TMDCs and how they change with intercalation make it difficult to check the accuracy of our calculations with other first principles works, investigations using other theoretical approaches, and with experimental works. We have therefore performed a separate study into graphite and LiCoO<sub>2</sub> (for which there are several works in the literature) to determine the reliability of our results, which we present here.

### 1. Graphite Results

The elastic tensor for AB stacked graphite was calculated using k-point grids of  $18 \times 18 \times 9$  (2,916 total, 185 irreducible),  $24 \times 24 \times 12$  (6,912 total, 427 irreducible), and  $30 \times 30 \times 15$  (13,500 total, 728 irreducible). More k-points are used in the grids compared to the TMDCs presented in the main article due to the smaller lattice constant of graphite. However, the density of k-points used for the study of graphite is comparable to the density of k-points used for the study of the TMDCs.

The elements of the tensor, along with values found within literature, are presented in Table SII. As can be seen, for the tensor elements of  $c_{11}$ ,  $c_{12}$ ,  $c_{33}$ , and  $c_{66}$  the difference between the higher k-point grids considered and the experiment and other theoretical results is small. Disagreement between experiment and calculations is observed in the values of  $c_{13}$  and  $c_{44}$ . For  $c_{13}$  the range of theoretical data and the choice of approach presents a large range of values with the only measured value being provided by sonic scattering. Similarly, the  $c_{44}$  value shows a similar range. Critically, all the data presented shows that the minimum k-point density required corresponds to the  $24 \times 24 \times 12$  grid (which is similar to that we have

Method	c <sub>11</sub> (GPa)	c <sub>12</sub> (GPa)	c <sub>13</sub> (GPa)	c <sub>33</sub> (GPa)	c <sub>44</sub> (GPa)	c <sub>66</sub> (GPa)
Our work 18 × 18 × 9	1042.98	216.83	-2.99	32.32	-0.24	413.07
Our work 24 × 24 × 12	1038.40	221.40	-2.98	32.37	1.45	408.50
Our work 30 × 30 × 15	1051.02	208.75	-2.96	32.29	2.54	421.14
LDA <sup>21</sup>	1104.8	203.9	2.5	30.9	5.6	450.45
LDA <sup>18</sup>	1105	204	2.5	30.9	5.6	450
LDA <sup>26</sup>	1037.7(2.4)	180.8(1.6)	-12.4(0.3)	22.7(0.6)	1.2(0.5)	428.4
GGA-PBE <sup>26</sup>	1036.3(2.4)	170.3(1.4)	-12.4(0.2)	39.8(0.6)	3.3(0.5)	432.9
Lattice dynamics <sup>27</sup>	1211.3	275.5	0.59	36.79	4.18	468.0
Lattice dynamics <sup>28</sup>	1060	180	15	36.5	4.0	440
Lattice dynamics <sup>29</sup>	1130	354	-	37.4	4.4	388
Lattice dynamics <sup>30</sup>	1060	160	15	36.9	4.2	450
Sonic resonance <sup>31,32</sup>	1060(20)	180(20)	15(5)	36.5(1.0)	4.0	440
Neutron scattering <sup>33</sup>	-	-	-	-	3.8(0.4)	-
Neutron scattering <sup>34</sup>	-	-	-	37.1(0.5)	-	-
Brillouin scattering <sup>35</sup>	-	-	-	-	5.05(0.35)	-

Table S II: Comparison of graphite elastic matrix elements calculated in this work and obtained from literature. The numbers in parentheses are error estimates in GPa. Some elements not explicitly written in the provided sources have been included using

$$c_{66} = \frac{1}{2}(c_{11} - c_{12}).$$

adopted for the TMDCs). From these elastic tensor elements we can obtain several elastic properties, as given by the discussions of the main article. We present these in Table SIII, where we see close agreement with literature values.

Method	Bulk Modulus (GPa)			Shear Modulus (GPa)			Young's Modulus (GPa)			Poisson Ratio			Pugh Ratio		
	V	R	H	V	R	H	V	R	H	V	R	H	V	R	H
Our work 18 × 18 × 9	282.22	30.46	156.34	209.68	-0.60	104.54	504.18	-1.80	256.46	0.20	0.51	0.23	1.35	-50.96	1.50
Our work 24 × 24 × 12	282.23	30.50	156.36	208.53	3.50	106.01	501.95	10.11	259.41	0.20	0.44	0.22	1.35	8.72	1.47
Our work 30 × 30 × 15	282.22	30.43	156.33	214.01	6.01	110.01	512.49	16.91	267.32	0.20	0.41	0.21	1.32	5.07	1.42
LDA <sup>21</sup>	295.37	29.71	162.54	227.77	12.33	120.05	543.58	32.50	289.00	0.19	0.32	0.20	1.30	2.41	1.35
LDA <sup>18</sup>	295.43	29.71	162.57	227.80	12.33	120.07	543.67	32.50	289.04	0.19	0.32	0.21	1.30	2.41	1.35
LDA <sup>26</sup>	267.79	20.82	144.31	215.64	2.89	109.27	510.03	8.29	261.74	0.18	0.43	0.20	1.24	7.21	1.32
GGA-PBE <sup>26</sup>	267.04	35.72	151.38	219.05	7.76	113.40	516.04	21.71	272.23	0.18	0.40	0.20	1.22	4.60	1.33
Lattice dynamics <sup>27</sup>	334.75	35.11	184.93	240.77	9.63	125.20	582.62	26.46	306.44	0.21	0.37	0.22	1.39	3.65	1.48
Lattice dynamics <sup>28</sup>	286.28	35.76	161.02	219.37	9.21	114.29	524.21	25.45	277.27	0.19	0.38	0.21	1.31	3.88	1.41
Lattice dynamics <sup>30</sup>	281.88	36.12	159.00	222.81	9.64	116.22	529.03	26.56	280.36	0.19	0.38	0.21	1.27	3.75	1.39
Sonic resonance <sup>31,32</sup>	286.28	35.76	161.02	219.37	9.21	114.29	524.21	25.45	277.27	0.19	0.38	0.21	1.31	3.88	1.41

Table S III: Comparison of graphite elastic values calculated in this work and obtained from literature. Values have been calculated using the elements of the elastic matrix presented in Table SII.

## 2. Lithium Cobalt Oxide Results

The elastic tensor for LiCoO<sub>2</sub> was calculated using k-point grids of  $12 \times 12 \times 4$  (576 total, 164 irreducible),  $18 \times 18 \times 6$  (1,944 total, 202 irreducible), and  $24 \times 24 \times 8$  (4,608 total, 449 irreducible). Fewer k-points are used along the  $\mathbf{k}_c$  direction compared to the TMDCs presented in the main article due to the larger lattice constant of LiCoO<sub>2</sub>. However, the density of k-points used for the study of LiCoO<sub>2</sub> is comparable to the density of k-points used for the study of the TMDCs. The elements of the tensor, along with values found within literature, are presented in Table SIV. We then compare in Table SV various elastic values calculated in this work and presented in literature.

In contrast to graphite, for LiCoO<sub>2</sub> experimental values of many of the elastic elements could not be found. Thus we limit our comparison of the elements of the tensor to strict comparison with other calculations, as presented in Table SIV. As can be seen, for the tensor elements of  $c_{11}$ ,  $c_{12}, c_{13}$   $c_{33}$ ,  $c_{44}$ , and  $c_{66}$  the difference between the higher k-point grids considered and other theoretical first principle results is small. Disagreement between various methods arises in the value of  $c_{14}$ . In our results, the variation in  $c_{14}$  with k-point density is very small and whilst it captures the negative value shown in several works, the precise value is open to contention. Again, as noted for graphite, the data presented shows that the k-point density  $18 \times 18 \times 6$  grid (which is similar to that we have adopted for the TMDCs) is more than sufficient. Given the natural structural comparisons between LiCoO<sub>2</sub> and the TMDCs this provides the basis for our k-point grid choice. From these elastic tensor elements we can obtain several elastic properties, as given by the discussions of the main article. We present these in Table SV, where we see that our results demonstrate small deviations from the experimentally measured values, with the Reuss scheme generally being the closest to the experimentally derived values.

Method	c <sub>11</sub> (GPa)	c <sub>12</sub> (GPa)	c <sub>13</sub> (GPa)	c <sub>33</sub> (GPa)	c <sub>44</sub> (GPa)	c <sub>14</sub> (GPa)	c <sub>66</sub> (GPa)
Our work 12 × 12 × 4	362.10	107.44	72.00	227.92	60.13	-2.11	127.33
Our work 18 × 18 × 6	359.68	106.27	70.33	225.70	58.65	-2.58	126.71
Our work 24 × 24 × 8	362.03	107.37	71.90	227.78	60.12	-2.11	127.33
HSE <sup>18</sup>	422	106	62	239	68.1	0	158
Materials Project <sup>36</sup>	233	104	51	196	30	-46	65
PBE <sup>37</sup>	339.79	101.6	65.78	214.67	51.47	6.39	119.10
GULP <sup>38</sup>	596.4	199.4	133.5	375.2	124.1	-8.28	198.5
GULP <sup>38</sup>	569.9	185.2	87.8	313.8	68.0	-33.6	192.3

Table S IV: Comparison of LiCoO<sub>2</sub> elastic matrix elements calculated in this work and obtained from literature. Some elements not explicitly written in the provided sources have been included using  $c_{66} = \frac{1}{2}(c_{11} - c_{12})$ .

Method	Bulk Modulus (GPa)			Shear Modulus (GPa)			Young's Modulus (GPa)			Poisson Ratio			Pugh Ratio		
	V	R	H	V	R	H	V	R	H	V	R	H	V	R	H
Our work $12 \times 12 \times 4$	161.67	151.63	156.65	96.23	84.69	90.46	240.89	214.20	227.57	0.25	0.26	0.26	1.68	1.79	1.73
Our work $18 \times 18 \times 6$	159.88	149.79	154.83	95.34	83.33	89.34	238.60	210.89	224.78	0.25	0.27	0.26	1.68	1.80	1.73
Our work $24 \times 24 \times 8$	161.58	151.53	156.55	96.23	84.69	90.46	240.86	214.17	227.55	0.25	0.26	0.26	1.68	1.79	1.73
HSE <sup>18</sup>	171	156	163	115	98.6	107	283	244	264	0.22	0.24	0.23	1.48	1.58	1.53
LDA <sup>39</sup>	168.5 (EOS)			-	-	-	-	-	-	-	-	-	-	-	-
GGA <sup>39</sup>	142.9 (EOS)			-	-	-	-	-	-	-	-	-	-	-	-
Nanoindentation <sup>40</sup>	-	-			-			191 (10)			-			-	
Pulse echo <sup>40</sup>	-	80 (1)			198 (2)			0.24			-			-	
XRD <sup>39</sup>	149 (20)			-			-			-			-		
Nanoindentation <sup>41</sup>	-	-			174 (25)			-			-			-	

Table S V: Comparison of LiCoO<sub>2</sub> elastic values calculated in this work and obtained from literature. The numbers in parentheses are error estimates. EOS indicates values calculated by fitting an equation of state, and not using the V/R/H methods.

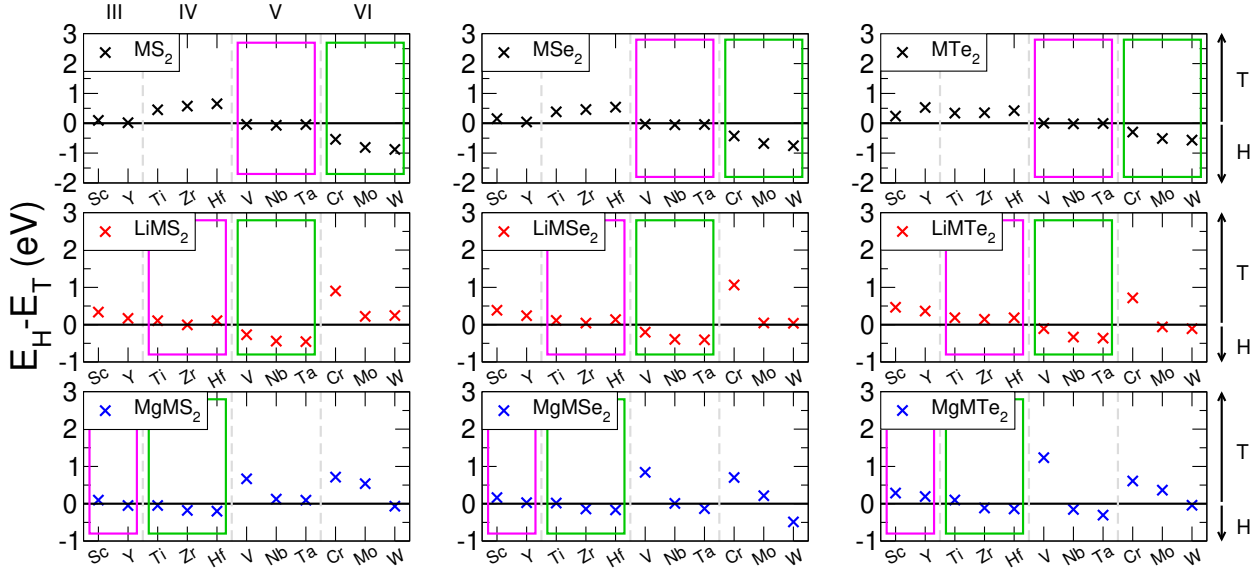


Figure S 1: Comparison of the TMDC T- and H-phase energies for the sulfides (left), selenides (middle), and tellurides (right). Data for pristine bulk structures is presented in black, lithium-intercalated structures in red, and magnesium-intercalated structures in blue. Positive values indicate a more favourable T-phase, whereas negative values indicate a more favourable H-phase. Group V-like behaviour is tracked with the magenta boxes, and Group VI-like behaviour is tracked with the green boxes.

### C. Summary of Previous Work

#### 1. Comparison of T-Phase and H-Phase TMDCs

Our previous work<sup>42</sup> evaluated the energetic ordering of the T- and H-phase TMDCs by taking the difference between the H-phase energy ( $E_H$ ) and the T-phase energy ( $E_T$ ). The number of transition metal  $d$ -electrons determines the preferred phase for a given TMDC, and so charge donation from the intercalated species can change the preferred phase by changing the effective number of  $d$ -electrons on the transition metal. This has been demonstrated by many materials, but most notably by MoS<sub>2</sub><sup>43,44</sup>. Our larger study found that the H-phase is relevant only for pristine Group VI TMDCs, lithium-intercalated Group V TMDCs, and magnesium-intercalated Group IV TMDCs. The results for these are shown in Figure S1, where positive values indicate the T-phase is more favourable and negative values indicate the H-phase is more favourable.

With lithium intercalation, we note that the electron count of Group VI metal sulfides

has effectively increased by one, resulting in them being ‘Group VII-like’ and reproducing the  $\text{H} \rightarrow \text{T}$  transition seen in  $\text{MoS}_2$ . When Group V materials are intercalated with lithium the extra electron results in ‘Group VI-like’ behaviour (with the H phase being preferred), and upon magnesium intercalation the Group IV materials become ‘Group VI-like’. This behaviour, and the favourability of the H-phase over the T-phase, is indicated with the green boxes in Figure S1. We see that the pristine Group V materials show little difference in energy between the T- and H-phase (with  $E_H - E_T$  being close to 0 eV). When intercalated with lithium, the Group IV materials lose their clear preference for the T-phase and become ‘Group V-like’, as do the Group III materials when intercalated with magnesium. However, as these energy differences remain relatively small, the T-phase is determined to be of the most interest due to the preference of the wider TMDC family to exhibit it, the relevance of the T-phase even for those TMDCs which adopt the H-phase at some point, and for ease of comparison of results between the different TMDCs considered in this work. Hence, we only consider the T-phase here.

## 2. Intercalation Stability

There are two metrics that can be used to assess the stability of a host TMDC with intercalation. The first is the formation energy, given by,

$$E_{\text{form}} = E_{\text{LiMX}_2} - [E_{\text{MX}_2} + E_{\text{Li}}], \quad (\text{S1})$$

where  $E_{\text{MX}_2}$  is the energy of the pristine bulk  $\text{MX}_2$  structure,  $E_{\text{LiMX}_2}$  is the energy of the intercalation  $\text{MX}_2$  structure, and  $E_{\text{Li}}$  is the energy of a lithium atom as found in bulk. An equivalent expression can be written for magnesium intercalated TMDCs. We present in Figure S2a and Figure S2b the formation energy (per formula unit) for the lithium-intercalated and magnesium-intercalated TMDCs, respectively. We see that all TMDCs (with the exception of magnesium-intercalated  $\text{TaTe}_2$ ) show negative formation energies, and therefore intercalation is energetically favourable.

An alternative metric for discussing the stability of TMDCs with intercalation is provided with  $E_{IS}$ , a detailed description of which has been provided previously<sup>42</sup>.  $E_{IS}$  describes the competition between the intercalated TMDC structure, the pristine bulk  $\text{MX}_2$  compound,

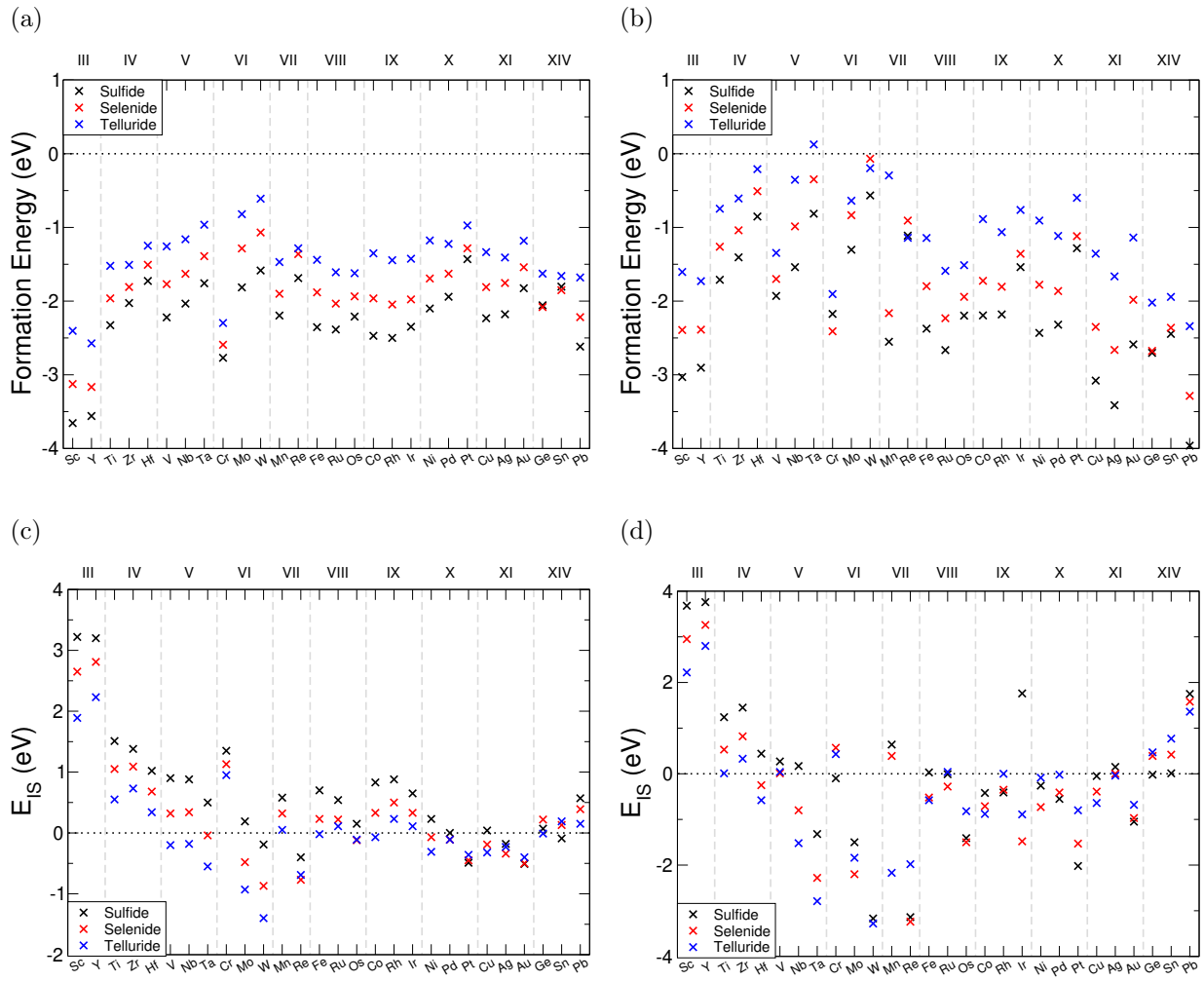


Figure S 2: Metrics used to assess the stability of TMDCs when intercalated with lithium and magnesium. The formation energy (per formula unit) described by equation (S1) is presented in S2a for lithium and in S2b for magnesium. Negative values of formation energy indicate intercalation is favourable. The stability against conversion into  $\text{Li}_2\text{X}$  or  $\text{MgX}$  can be described through  $E_{IS}$  given by equations (S2) and (S3). This is presented in S2c for lithium and in S2d for magnesium. Positive values of formation energy indicate intercalation is favourable. In each, sulfide data is presented in black, selenide data is presented in red, and telluride data is presented in blue.

and commonly-observed conversion products. It is given in terms of the enthalpy of formation values,  $\Delta H$ , for different compounds and the concentration  $a$  (for our discussion,  $a = 1$ ) of an intercalant in the host TMDC. For lithium, this is,

$$E_{IS}^{\text{Li}} = \frac{2}{4-a} \Delta H(\text{Li}_2\text{X}) + \frac{1}{a} \Delta H(\text{MX}_2) - \frac{4}{4a-a^2} \Delta H(\text{Li}_a\text{MX}_2), \quad (\text{S2})$$

and for magnesium intercalation, we have an equivalent expression,

$$E_{IS}^{\text{Mg}} = \frac{2}{2-a} \Delta H(\text{MgX}) + \frac{1}{a} \Delta H(\text{MX}_2) - \frac{2}{2a-a^2} \Delta H(\text{Mg}_a\text{MX}_2). \quad (\text{S3})$$

In the context of a thermodynamic phase diagram, larger positive values of  $E_{IS}$  indicate a larger region on the phase diagram corresponding to a stable  $\text{LiMX}_2$  or  $\text{MgMX}_2$  structure. Smaller positive values suggest a reduced stability, and negative values indicate a material is susceptible to a conversion reaction into  $\text{Li}_2\text{X}$  or  $\text{MgX}$  and the consequent loss of the layered structure.

We present in Figure S2c and Figure S2d the values of  $E_{IS}$  for the lithium-intercalated and magnesium-intercalated TMDCs, respectively. Most TMDCs show positive values of  $E_{IS}^{\text{Li}}$ , with a few selenide and telluride materials showing negative values. Near all TMDCs show negative values  $E_{IS}^{\text{Mg}}$ , and this reduction in stability has previously been attributed to the extra charge transferred from the magnesium intercalant compared to lithium. However, whilst negative values of  $E_{IS}$  indicate an intercalated TMDC material is susceptible to conversion reactions, it does not need occur instantaneously. In several cases, the intercalated TMDC is metastable, being able to offer some electrode cycling before conversion occurs on a significant scale. Further, if the intercalated structure were to be used in an application other than as intercalation electrode which involved less dynamic ionic motion, it could be expected that the intercalated TMDC could retain its layered structure due to a lack of driving force disturbing the metastable state.

## II. RESULTS

### A. Single Crystal Bulk Modulus

In the main article we presented the single crystal bulk modulus for each of the pristine and intercalated TMDC structures. These were obtained by extending and compressing the lattice vectors by 0%,  $\pm 1\%$ ,  $\pm 2\%$ , and fitting the resulting energies with a quadratic. In the following tables, we present the numerical values of the bulk modulus obtained this way, along with the  $R^2$  values arising from the fit. Table SVI, Table SVII, and Table SVIII contain the results for the pristine, lithium-intercalated, and magnesium-intercalated structures, respectively.

We find that most of the fits show  $R^2$  values greater than 0.99. Of those that fall below this value, seven ( $\text{MoS}_2$ ,  $\text{ReS}_2$ ,  $\text{ScSe}_2$ ,  $\text{VTe}_2$ ,  $\text{NbTe}_2$ ,  $\text{LiVTe}_2$ , and  $\text{MgMnTe}_2$ ) are in the range  $R^2 = 0.98 - 0.99$ . A further eleven fall below  $R^2 = 0.98$ , but these are either found to be elastically unstable (such as  $\text{LiMnSe}_2$ ,  $\text{MgMnS}_2$ , and  $\text{MgCrSe}_2$ , see Section SII C) or demonstrate a range of magnetic moments at different strains (such as  $\text{MnSe}_2$ ,  $\text{OsSe}_2$ ,  $\text{CrTe}_2$ ,  $\text{LiCrTe}_2$ ,  $\text{LiMnTe}_2$ ,  $\text{LiVSe}_2$ , and  $\text{MgMnSe}_2$ ) hence making a quadratic fit inappropriate. However, for consistency, we have maintained this approach in the main article, whilst highlighting the issues arising from these magnetic considerations.

M	Sulfides		Selenides		Tellurides	
	Bulk Mod (GPa)	R <sup>2</sup>	Bulk Mod (GPa)	R <sup>2</sup>	Bulk Mod (GPa)	R <sup>2</sup>
Sc	36.86	0.9962	31.95	0.9898	24.87	0.9932
Y	38.28	0.9965	31.19	0.9940	22.37	0.9918
Ti	43.24	0.9983	37.42	0.9939	32.17	0.9933
Zr	42.74	0.9977	35.26	0.9980	25.74	0.9914
Hf	46.20	0.9978	38.25	0.9978	26.03	0.9908
V	45.58	0.9963	41.48	0.9936	32.62	0.9804
Nb	50.13	0.9956	44.80	0.9939	37.74	0.9869
Ta	54.68	0.9976	43.92	0.9955	37.56	0.9931
Cr	57.62	0.9960	49.33	0.9961	152.97	0.9276
Mo	60.99	0.9885	55.91	0.9945	43.49	0.9951
W	57.43	0.9949	57.06	0.9938	43.29	0.9946
Mn	31.70	0.9998	132.02	0.9419	41.70	0.9904
Re	46.47	0.9807	55.30	0.9943	53.54	0.9938
Fe	44.85	0.9962	54.16	0.9942	46.35	0.9925
Ru	61.08	0.9953	64.56	0.9939	64.44	0.9952
Os	63.98	0.9963	61.64	0.9171	65.72	0.9939
Co	73.93	0.9936	67.58	0.9924	59.13	0.9935
Rh	77.62	0.9948	75.55	0.9939	67.15	0.9935
Ir	84.10	0.9957	77.69	0.9950	70.58	0.9917
Ni	80.84	0.9958	74.73	0.9934	66.88	0.9944
Pd	82.76	0.9954	82.36	0.9939	73.30	0.9935
Pt	86.21	0.9964	85.78	0.9956	78.29	0.9952
Cu	98.03	0.9968	87.79	0.9964	70.38	0.9961
Ag	92.28	0.9962	81.50	0.9956	64.64	0.9963
Au	103.92	0.9947	95.12	0.9954	74.86	0.9950
Ge	49.47	0.9973	41.19	0.9965	56.50	0.9960
Sn	41.49	0.9972	35.70	0.9973	52.57	0.9940
Pb	58.37	0.9961	54.47	0.9962	46.52	0.9963

Table S VI: Single crystal bulk modulus values and the corresponding R<sup>2</sup> values for the quadratic fits for pristine TMDCs.

M	Sulfides		Selenides		Tellurides	
	Bulk Mod (GPa)	R <sup>2</sup>	Bulk Mod (GPa)	R <sup>2</sup>	Bulk Mod (GPa)	R <sup>2</sup>
Sc	60.45	0.9971	51.56	0.9974	40.24	0.9978
Y	49.42	0.9970	43.90	0.9970	35.20	0.9975
Ti	72.60	0.9975	54.85	0.9954	40.97	0.9964
Zr	68.83	0.9971	59.13	0.9974	46.01	0.9971
Hf	74.79	0.9970	63.32	0.9972	48.04	0.9965
V	81.00	0.9970	60.63	0.9328	47.27	0.9874
Nb	81.61	0.9963	69.68	0.9966	53.49	0.9955
Ta	87.70	0.9962	73.40	0.9963	55.30	0.9942
Cr	69.80	0.9971	58.95	0.9974	148.85	0.9416
Mo	88.92	0.9964	68.79	0.9950	55.50	0.9954
W	95.05	0.9964	72.18	0.9940	54.39	0.9947
Mn	78.44	0.9976	96.42	0.6334	162.56	0.9037
Re	79.12	0.9977	69.56	0.9977	60.96	0.9969
Fe	83.23	0.9972	69.14	0.9973	57.87	0.9976
Ru	83.71	0.9976	73.73	0.9976	64.61	0.9965
Os	86.22	0.9972	74.55	0.9962	69.43	0.9967
Co	87.47	0.9972	72.31	0.9974	60.75	0.9973
Rh	84.43	0.9974	73.24	0.9975	63.99	0.9968
Ir	91.95	0.9975	80.57	0.9974	69.17	0.9967
Ni	71.39	0.9954	60.87	0.9911	52.87	0.9953
Pd	69.00	0.9947	62.12	0.9944	60.85	0.9957
Pt	74.69	0.9967	66.25	0.9933	64.04	0.9953
Cu	70.67	0.9901	64.15	0.9961	54.85	0.9965
Ag	66.36	0.9937	60.84	0.9961	51.49	0.9957
Au	69.53	0.9917	66.64	0.9945	58.97	0.9962
Ge	54.97	0.9943	46.88	0.9959	40.97	0.9905
Sn	47.82	0.9955	42.54	0.9972	35.47	0.9962
Pb	44.15	0.9965	39.50	0.9970	33.37	0.9967

Table S VII: Single crystal bulk modulus values and the corresponding R<sup>2</sup> values for the quadratic fits for lithium-intercalated TMDCs.

M	Sulfides		Selenides		Tellurides	
	Bulk Mod (GPa)	R <sup>2</sup>	Bulk Mod (GPa)	R <sup>2</sup>	Bulk Mod (GPa)	R <sup>2</sup>
Sc	90.55	0.9967	74.27	0.9968	56.89	0.9970
Y	84.38	0.9970	70.33	0.9970	52.95	0.9964
Ti	101.72	0.9970	78.07	0.9917	42.72	0.9979
Zr	106.41	0.9970	86.26	0.9970	64.80	0.9969
Hf	112.54	0.9965	89.58	0.9964	64.47	0.9967
V	91.34	0.9980	76.51	0.9967	61.45	0.9972
Nb	120.27	0.9970	94.42	0.9968	70.32	0.9967
Ta	124.61	0.9963	92.42	0.9956	68.60	0.9969
Cr	25.40	0.9822	156.48	0.8200	59.17	0.9968
Mo	125.30	0.9952	88.04	0.9974	72.78	0.9971
W	121.32	0.9944	89.21	0.9969	75.05	0.9969
Mn	143.79	0.7669	187.8	0.9119	61.186	0.9818
Re	115.07	0.9972	96.48	0.9971	83.25	0.9970
Fe	90.09	0.9975	96.95	0.9972	77.24	0.9968
Ru	121.03	0.9972	102.76	0.9969	83.37	0.9970
Os	125.43	0.9971	106.70	0.9970	90.74	0.9969
Co	105.51	0.9967	88.16	0.9970	70.73	0.9967
Rh	105.13	0.9966	90.91	0.9961	74.83	0.9964
Ir	108.60	0.9972	95.71	0.9965	80.07	0.9958
Ni	92.41	0.9978	78.01	0.9980	68.84	0.9960
Pd	97.59	0.9961	83.74	0.9955	67.49	0.9967
Pt	101.99	0.9961	83.45	0.9950	72.58	0.9965
Cu	88.20	0.9972	71.65	0.9932	57.87	0.9965
Ag	76.13	0.9957	65.77	0.9954	53.86	0.9964
Au	84.57	0.9947	72.24	0.9954	59.94	0.9968
Ge	72.12	0.9975	61.72	0.9965	40.18	0.9729
Sn	66.28	0.9974	57.25	0.9972	45.72	0.9972
Pb	65.25	0.9972	56.11	0.9970	44.56	0.9969

Table S VIII: Single crystal bulk modulus values and the corresponding R<sup>2</sup> values for the quadratic fits for magnesium-intercalated TMDCs.

### B. Elastic Tensors

Here, we present the space group number and the elements of the elastic matrix for each of the pristine TMDCs (Table SIX, Table SX and Table SXI), as well as the lithium-intercalated (Table SXII, Table SXIII and Table SXIV) and magnesium-intercalated (Table SXV, Table SXVI and Table SXVII) structures. We only specify the elements  $c_{11}$ ,  $c_{12}$ ,  $c_{13}$ ,  $c_{33}$ ,  $c_{44}$ ,  $c_{14}$ , and  $c_{66}$ , as these are the unique non-zero elements for elastic matrices of materials with a space group of 164. The only material we find to possess a different space group number is LiCrS<sub>2</sub>, the elastic matrix of which is:

$$\begin{pmatrix} 154.56 & 45.63 & 31.65 & 6.38 & 0.06 & 0.03 \\ . & 154.07 & 31.33 & -5.91 & 0.04 & 0.03 \\ . & . & 111.09 & 0.29 & 0.07 & 0.04 \\ . & . & . & 37.50 & 0.01 & 0.00 \\ . & . & . & . & 37.58 & 6.16 \\ . & . & . & . & . & 54.36 \end{pmatrix}. \quad (\text{S4})$$

MS <sub>2</sub>	Space Group	c <sub>11</sub> (GPa)	c <sub>12</sub> (GPa)	c <sub>13</sub> (GPa)	c <sub>33</sub> (GPa)	c <sub>44</sub> (GPa)	c <sub>14</sub> (GPa)	c <sub>66</sub> (GPa)
ScS <sub>2</sub>	164	62.99	26.62	21.32	40.70	-14.35	-3.58	18.18
YS <sub>2</sub>	164	67.44	37.43	21.19	44.87	-17.20	-5.40	15.00
TiS <sub>2</sub>	164	137.22	26.95	7.87	32.77	11.39	3.21	55.13
ZrS <sub>2</sub>	164	134.21	26.51	7.65	34.19	8.57	2.43	53.85
HfS <sub>2</sub>	164	147.31	28.62	7.92	34.31	9.14	2.74	59.35
VS <sub>2</sub>	164	158.94	17.04	10.62	30.33	13.45	5.31	70.95
NbS <sub>2</sub>	164	163.34	30.73	9.74	39.70	9.87	7.54	66.31
TaS <sub>2</sub>	164	173.42	32.02	7.63	37.77	13.89	4.44	70.70
CrS <sub>2</sub>	164	185.59	9.27	23.74	41.04	11.49	5.31	88.29
MoS <sub>2</sub>	164	178.15	1.82	30.76	24.84	13.39	7.22	88.16
WS <sub>2</sub>	164	199.47	12.07	25.58	36.96	13.74	6.84	93.70
MnS <sub>2</sub>	164	92.60	16.12	14.43	16.59	6.43	3.83	38.24
ReS <sub>2</sub>	164	147.87	-1.81	34.32	39.73	7.89	4.25	74.84
FeS <sub>2</sub>	164	92.92	64.12	19.59	28.71	7.76	4.75	14.40
RuS <sub>2</sub>	164	107.25	104.09	22.07	87.53	33.66	9.04	1.58
OsS <sub>2</sub>	164	121.01	105.97	22.45	73.39	22.10	3.96	7.52
CoS <sub>2</sub>	164	152.13	91.22	29.41	87.47	22.19	1.69	30.45
RhS <sub>2</sub>	164	136.37	91.17	31.29	105.07	17.13	-12.72	22.60
IrS <sub>2</sub>	164	194.20	91.50	26.60	89.14	25.84	-0.42	51.35
NiS <sub>2</sub>	164	202.99	63.52	36.23	81.67	31.00	15.15	69.73
PdS <sub>2</sub>	164	190.72	65.27	44.57	81.57	38.80	18.75	62.73
PtS <sub>2</sub>	164	239.75	66.27	29.95	38.81	50.97	27.93	86.74
CuS <sub>2</sub>	164	166.44	56.57	70.64	152.04	59.32	18.72	54.93
AgS <sub>2</sub>	164	141.15	65.25	72.87	119.28	49.10	15.61	37.95
AuS <sub>2</sub>	164	173.48	83.32	67.80	122.20	52.98	8.85	45.08
GeS <sub>2</sub>	164	149.70	39.30	9.51	30.51	8.87	-0.97	55.20
SnS <sub>2</sub>	164	120.30	31.13	10.07	25.27	7.88	0.79	44.58
PbS <sub>2</sub>	164	68.00	61.98	47.30	74.79	-21.32	-21.67	3.01

Table S IX: Elements of the elastic matrix for pristine TMDC sulfides.

MSe <sub>2</sub>	Space	c <sub>11</sub>	c <sub>12</sub>	c <sub>13</sub>	c <sub>33</sub>	c <sub>44</sub>	c <sub>14</sub>	c <sub>66</sub>
	Group	(GPa)						
ScSe <sub>2</sub>	164	50.31	18.42	22.29	35.14	-10.70	-1.23	15.94
YSe <sub>2</sub>	164	54.06	28.14	20.82	39.16	-15.19	-3.87	12.96
TiSe <sub>2</sub>	164	101.21	21.14	13.42	24.01	11.82	4.07	40.04
ZrSe <sub>2</sub>	164	108.49	22.15	6.70	32.62	9.50	2.65	43.17
HfSe <sub>2</sub>	164	118.92	23.81	6.99	32.64	9.74	2.84	47.56
VSe <sub>2</sub>	164	116.37	14.94	13.72	24.44	12.11	5.53	50.71
NbSe <sub>2</sub>	164	140.09	25.64	10.55	39.59	18.53	7.05	57.22
TaSe <sub>2</sub>	164	136.33	23.76	9.96	34.65	12.95	5.01	56.28
CrSe <sub>2</sub>	164	148.02	15.20	21.77	38.73	9.90	4.24	66.41
MoSe <sub>2</sub>	164	165.10	4.80	24.97	33.93	8.76	6.19	80.15
WSe <sub>2</sub>	164	173.30	2.63	28.28	41.38	4.12	4.34	85.34
MnSe <sub>2</sub>	164	209.20	155.40	245.75	294.47	9.18	-1.72	26.90
ReSe <sub>2</sub>	164	175.63	-2.66	27.38	57.75	5.40	4.23	89.14
FeSe <sub>2</sub>	164	14.08	150.88	29.89	39.82	9.90	28.92	-68.40
RuSe <sub>2</sub>	164	79.20	73.87	36.96	89.40	32.75	10.63	2.67
OsSe <sub>2</sub>	164	119.61	79.26	31.10	75.38	31.81	11.90	20.18
CoSe <sub>2</sub>	164	123.53	79.66	38.11	67.24	20.61	10.12	21.94
RhSe <sub>2</sub>	164	103.91	97.55	41.52	92.49	12.18	-9.51	3.18
IrSe <sub>2</sub>	164	148.22	89.03	32.29	86.83	24.18	-0.14	29.59
NiSe <sub>2</sub>	164	163.57	58.39	41.88	87.64	22.19	10.20	52.59
PdSe <sub>2</sub>	164	140.57	66.95	51.53	87.74	19.60	3.82	36.81
PtSe <sub>2</sub>	164	202.57	65.19	42.91	62.58	47.52	25.49	68.69
CuSe <sub>2</sub>	164	146.67	53.43	64.75	131.00	51.48	20.98	46.62
AgSe <sub>2</sub>	164	123.72	56.42	69.03	98.32	45.04	19.72	33.65
AuSe <sub>2</sub>	164	154.01	69.11	71.80	111.87	54.71	19.57	42.45
GeSe <sub>2</sub>	164	99.10	39.22	13.43	28.98	7.67	-1.06	29.94
SnSe <sub>2</sub>	164	97.63	26.17	12.36	23.25	7.68	0.98	35.73
PbSe <sub>2</sub>	164	48.16	67.06	49.61	66.57	-19.93	-25.70	-9.45

Table S X: Elements of the elastic matrix for pristine TMDC selenides.

MTe <sub>2</sub>	Space	c <sub>11</sub> (GPa)	c <sub>12</sub> (GPa)	c <sub>13</sub> (GPa)	c <sub>33</sub> (GPa)	c <sub>44</sub> (GPa)	c <sub>14</sub> (GPa)	c <sub>66</sub> (GPa)
	Group							
ScTe <sub>2</sub>	164	32.21	21.89	18.06	38.68	1.77	2.85	5.16
YTe <sub>2</sub>	164	28.44	13.22	18.22	34.22	-8.76	-0.85	7.61
TiTe <sub>2</sub>	164	77.49	18.02	12.83	35.47	17.16	6.15	29.73
ZrTe <sub>2</sub>	164	65.99	11.13	8.54	33.97	13.74	4.88	27.43
HfTe <sub>2</sub>	164	67.86	10.47	8.81	29.17	13.69	4.66	28.70
VTe <sub>2</sub>	164	81.22	19.69	17.51	28.92	20.58	7.97	30.77
NbTe <sub>2</sub>	164	110.17	22.89	15.87	31.75	21.90	11.54	43.64
TaTe <sub>2</sub>	164	104.86	22.42	15.50	29.33	18.47	8.67	41.22
CrTe <sub>2</sub>	164	1178.75	1090.03	416.76	167.31	12.41	-0.33	44.36
MoTe <sub>2</sub>	164	127.06	4.83	21.10	33.18	5.17	3.48	61.12
WTe <sub>2</sub>	164	132.38	-2.40	22.27	36.15	3.45	3.20	67.39
MnTe <sub>2</sub>	164	67.93	19.45	26.26	45.70	13.80	10.99	24.24
ReTe <sub>2</sub>	164	103.30	47.97	33.12	53.36	33.30	16.05	27.66
FeTe <sub>2</sub>	164	77.79	52.30	21.17	50.31	23.82	10.56	12.74
RuTe <sub>2</sub>	164	117.81	59.68	33.55	78.74	33.22	14.80	29.06
OsTe <sub>2</sub>	164	119.30	74.66	31.99	70.36	30.02	15.33	22.32
CoTe <sub>2</sub>	164	125.67	52.96	30.95	62.23	23.08	10.24	36.36
RhTe <sub>2</sub>	164	104.04	63.69	43.29	79.63	20.63	6.06	20.17
IrTe <sub>2</sub>	164	143.75	65.12	37.79	78.59	40.30	18.31	39.31
NiTe <sub>2</sub>	164	135.20	42.51	41.69	88.59	28.16	14.83	46.35
PdTe <sub>2</sub>	164	88.76	89.62	50.69	85.07	-35.79	-35.52	-0.43
PtTe <sub>2</sub>	164	152.45	49.16	39.41	72.58	46.72	20.37	51.65
CuTe <sub>2</sub>	164	111.11	38.93	56.61	103.60	41.99	17.94	36.09
AgTe <sub>2</sub>	164	96.05	41.41	55.95	76.77	37.07	19.92	27.32
AuTe <sub>2</sub>	164	124.42	49.54	61.80	92.96	48.64	21.94	37.44
GeTe <sub>2</sub>	164	68.28	44.77	50.08	75.99	12.59	2.91	11.75
SnTe <sub>2</sub>	164	65.55	37.51	45.57	62.17	5.06	4.11	14.02
PbTe <sub>2</sub>	164	59.49	40.13	42.00	46.30	2.75	-1.14	9.68

Table S XI: Elements of the elastic matrix for pristine TMDC tellurides.

LiMS <sub>2</sub>	Space Group	c <sub>11</sub> (GPa)	c <sub>12</sub> (GPa)	c <sub>13</sub> (GPa)	c <sub>33</sub> (GPa)	c <sub>44</sub> (GPa)	c <sub>14</sub> (GPa)	c <sub>66</sub> (GPa)
LiScS <sub>2</sub>	164	141.15	40.71	16.83	110.96	27.89	5.40	50.22
LiYS <sub>2</sub>	164	120.77	34.11	8.92	96.79	14.77	9.17	43.33
LiTiS <sub>2</sub>	164	160.33	37.30	31.19	129.00	47.94	2.23	61.51
LiZrS <sub>2</sub>	164	155.06	43.22	26.57	122.41	40.17	7.00	55.92
LiHfS <sub>2</sub>	164	165.26	45.92	30.58	129.02	43.38	7.44	59.67
LiVS <sub>2</sub>	164	166.11	30.06	49.75	129.97	57.89	0.09	68.02
LiNbS <sub>2</sub>	164	157.13	34.86	58.07	127.47	56.67	4.60	61.14
LiTaS <sub>2</sub>	164	108.03	80.92	66.35	130.02	58.16	9.40	13.55
LiCrS <sub>2</sub>	12	154.56	45.63	31.65	111.09	37.50	6.38	54.36
LiMoS <sub>2</sub>	164	172.21	36.69	63.13	132.12	60.94	3.75	67.76
LiWS <sub>2</sub>	164	178.15	39.02	66.60	141.49	57.33	3.62	69.57
LiMnS <sub>2</sub>	164	163.29	47.85	40.35	108.08	45.23	3.50	57.72
LiReS <sub>2</sub>	164	156.97	59.76	46.27	112.89	45.21	10.79	48.60
LiFeS <sub>2</sub>	164	89.52	143.02	42.01	106.06	45.23	5.60	-26.75
LiRuS <sub>2</sub>	164	160.77	88.63	36.89	108.70	42.83	6.01	36.07
LiOsS <sub>2</sub>	164	165.93	99.76	34.24	112.05	37.03	8.89	33.08
LiCoS <sub>2</sub>	164	196.89	59.95	42.55	103.13	43.27	4.73	68.47
LiRhS <sub>2</sub>	164	180.05	64.16	43.41	94.29	36.25	11.26	57.94
LiIrS <sub>2</sub>	164	212.04	70.13	40.93	99.70	35.36	12.54	70.95
LiNiS <sub>2</sub>	164	145.82	52.11	48.29	92.05	31.22	-3.13	46.86
LiPdS <sub>2</sub>	164	121.85	62.70	48.17	81.08	23.91	-0.21	29.58
LiPtS <sub>2</sub>	164	122.75	76.56	48.07	83.73	11.62	-9.18	23.10
LiCuS <sub>2</sub>	164	100.63	72.79	46.57	56.25	11.56	-19.09	13.92
LiAgS <sub>2</sub>	164	101.54	66.14	41.64	63.52	-2.38	-15.37	17.70
LiAuS <sub>2</sub>	164	81.85	94.77	44.62	65.43	-54.69	-51.14	-6.46
LiGeS <sub>2</sub>	164	108.02	49.75	23.29	103.24	25.76	0.50	29.14
LiSnS <sub>2</sub>	164	91.80	43.47	22.11	88.06	17.80	4.60	24.17
LiPbS <sub>2</sub>	164	71.42	45.61	19.43	80.50	9.98	1.80	12.91

Table S XII: Elements of the elastic matrix for lithium-intercalated TMDC sulfides.

LiMSe <sub>2</sub>	Space Group	c <sub>11</sub> (GPa)	c <sub>12</sub> (GPa)	c <sub>13</sub> (GPa)	c <sub>33</sub> (GPa)	c <sub>44</sub> (GPa)	c <sub>14</sub> (GPa)	c <sub>66</sub> (GPa)
LiScSe <sub>2</sub>	164	114.68	34.46	18.10	92.47	27.42	3.81	40.11
LiYSe <sub>2</sub>	164	101.32	29.84	11.98	84.38	18.75	7.17	35.74
LiTiSe <sub>2</sub>	164	118.04	26.57	31.26	101.47	41.81	1.48	45.73
LiZrSe <sub>2</sub>	164	123.58	32.45	28.97	100.10	39.63	4.86	45.57
LiHfSe <sub>2</sub>	164	131.28	36.54	31.38	103.26	40.76	5.52	47.37
LiVSe <sub>2</sub>	164	127.51	26.47	45.53	102.72	48.13	-0.47	50.52
LiNbSe <sub>2</sub>	164	131.61	25.92	51.35	102.87	49.73	3.53	52.85
LiTaSe <sub>2</sub>	164	106.63	47.08	57.86	102.05	50.17	5.09	29.77
LiCrSe <sub>2</sub>	164	125.75	38.95	30.22	86.08	33.82	5.00	43.40
LiMoSe <sub>2</sub>	164	113.27	28.22	64.12	98.97	46.99	2.00	42.53
LiWSe <sub>2</sub>	164	118.91	27.07	67.11	106.86	48.54	2.07	45.92
LiMnSe <sub>2</sub>	164	-291.01	-253.25	-1303.58	-3644.85	-1.29	-27.54	-18.88
LiReSe <sub>2</sub>	164	130.92	54.66	41.48	84.70	44.16	8.52	38.13
LiFeSe <sub>2</sub>	164	125.25	68.31	41.20	63.29	40.81	5.01	28.47
LiRuSe <sub>2</sub>	164	142.52	75.58	36.61	80.64	43.19	2.74	33.47
LiOsSe <sub>2</sub>	164	142.91	83.49	34.68	90.11	40.07	5.02	29.71
LiCoSe <sub>2</sub>	164	158.68	50.20	40.13	71.84	38.03	2.37	54.24
LiRhSe <sub>2</sub>	164	154.64	57.12	40.34	70.22	36.22	8.34	48.76
LiIrSe <sub>2</sub>	164	182.89	61.96	39.20	75.91	37.35	9.50	60.46
LiNiSe <sub>2</sub>	164	123.22	47.95	42.41	62.15	29.82	-2.76	37.63
LiPdSe <sub>2</sub>	164	115.63	59.63	43.94	58.66	25.54	-1.10	28.00
LiPtSe <sub>2</sub>	164	123.22	71.16	44.35	58.81	20.62	-6.58	26.03
LiCuSe <sub>2</sub>	164	107.96	58.14	43.01	57.89	14.04	-14.24	24.91
LiAgSe <sub>2</sub>	164	92.79	60.40	38.96	79.14	11.37	-9.42	16.19
LiAuSe <sub>2</sub>	164	103.31	65.08	40.62	70.48	-0.20	-13.36	19.12
LiGeSe <sub>2</sub>	164	83.59	46.16	23.00	82.12	24.14	1.37	18.72
LiSnSe <sub>2</sub>	164	76.32	39.06	22.22	69.91	19.05	3.70	18.63
LiPbSe <sub>2</sub>	164	59.70	41.02	20.02	66.76	7.57	-1.64	9.34

Table S XIII: Elements of the elastic matrix for lithium-intercalated TMDC selenides.

LiMTe <sub>2</sub>	Space Group	c <sub>11</sub> (GPa)	c <sub>12</sub> (GPa)	c <sub>13</sub> (GPa)	c <sub>33</sub> (GPa)	c <sub>44</sub> (GPa)	c <sub>14</sub> (GPa)	c <sub>66</sub> (GPa)
LiScTe <sub>2</sub>	164	82.18	26.54	18.82	69.07	26.30	2.47	27.82
LiYTe <sub>2</sub>	164	74.05	23.14	14.05	65.55	21.59	4.92	25.46
LiTiTe <sub>2</sub>	164	75.41	14.88	28.27	69.20	34.39	0.69	30.27
LiZrTe <sub>2</sub>	164	88.13	23.92	28.07	72.34	36.96	2.90	32.10
LiHfTe <sub>2</sub>	164	88.30	26.23	30.44	70.43	38.73	3.90	31.03
LiVTe <sub>2</sub>	164	88.21	18.33	43.08	77.96	39.39	-0.83	34.94
LiNbTe <sub>2</sub>	164	87.12	13.67	47.40	72.87	38.00	-0.25	36.72
LiTaTe <sub>2</sub>	164	89.50	13.60	50.36	72.43	37.19	1.60	37.95
LiCrTe <sub>2</sub>	164	505.04	452.73	515.94	69.53	29.41	-0.00	26.15
LiMoTe <sub>2</sub>	164	101.49	9.15	43.47	96.84	28.84	-2.93	46.17
LiWTe <sub>2</sub>	164	107.55	3.94	43.45	95.66	28.92	-2.93	51.80
LiMnTe <sub>2</sub>	164	42.13	2.36	528.09	2146.10	20.51	-3.35	19.88
LiReTe <sub>2</sub>	164	86.45	97.22	32.24	66.33	43.82	8.29	-5.38
LiFeTe <sub>2</sub>	164	110.50	57.36	32.32	53.07	43.39	-2.56	26.57
LiRuTe <sub>2</sub>	164	118.16	67.11	34.28	69.89	44.45	-1.71	25.52
LiOsTe <sub>2</sub>	164	139.74	67.70	33.56	74.45	45.18	-2.91	36.02
LiCoTe <sub>2</sub>	164	136.31	45.67	34.49	51.29	37.08	-3.48	45.32
LiRhTe <sub>2</sub>	164	138.51	55.24	36.23	54.70	39.60	2.17	41.63
LiIrTe <sub>2</sub>	164	161.49	55.97	32.98	48.02	41.73	4.15	52.76
LiNiTe <sub>2</sub>	164	103.44	44.20	37.85	35.94	26.07	-8.17	29.62
LiPdTe <sub>2</sub>	164	108.79	55.08	38.33	65.55	28.78	-4.55	26.86
LiPtTe <sub>2</sub>	164	121.71	56.74	37.55	59.37	29.12	-5.97	32.49
LiCuTe <sub>2</sub>	164	91.31	45.44	36.47	65.74	15.89	-10.86	22.93
LiAgTe <sub>2</sub>	164	75.06	48.92	33.28	70.85	13.01	-6.95	13.07
LiAuTe <sub>2</sub>	164	92.05	52.05	40.58	76.07	13.48	-7.59	20.00
LiGeTe <sub>2</sub>	164	49.66	43.12	26.15	54.60	18.94	-0.88	3.27
LiSnTe <sub>2</sub>	164	52.74	37.48	19.64	51.31	15.59	-0.32	7.63
LiPbTe <sub>2</sub>	164	37.73	38.40	25.07	44.27	2.95	-6.48	-0.33

Table S XIV: Elements of the elastic matrix for lithium-intercalated TMDC tellurides.

MgMS <sub>2</sub>	Space Group	c <sub>11</sub> (GPa)	c <sub>12</sub> (GPa)	c <sub>13</sub> (GPa)	c <sub>33</sub> (GPa)	c <sub>44</sub> (GPa)	c <sub>14</sub> (GPa)	c <sub>66</sub> (GPa)
MgScS <sub>2</sub>	164	157.67	49.81	56.05	188.68	64.71	6.78	53.93
MgYS <sub>2</sub>	164	141.85	45.61	56.20	165.50	59.62	12.33	48.12
MgTiS <sub>2</sub>	164	166.32	52.77	75.23	190.37	78.04	4.32	56.78
MgZrS <sub>2</sub>	164	174.74	55.67	79.04	187.41	78.22	7.32	59.54
MgHfS <sub>2</sub>	164	187.16	59.28	86.66	184.41	78.01	7.03	63.94
MgVS <sub>2</sub>	164	156.00	63.82	57.76	168.64	54.12	11.56	46.09
MgNbS <sub>2</sub>	164	182.36	61.73	95.52	208.69	86.41	6.32	60.31
MgTaS <sub>2</sub>	164	179.56	78.71	103.72	202.60	84.52	7.11	50.43
MgCrS <sub>2</sub>	164	158.78	74.42	38.67	1.89	69.86	6.07	42.18
MgMoS <sub>2</sub>	164	161.14	62.31	113.37	194.77	79.38	2.49	49.42
MgWS <sub>2</sub>	164	174.03	61.56	103.22	195.80	54.85	-11.22	56.24
MgMnS <sub>2</sub>	164	-211.31	-279.49	-1152.05	-3222.03	20.88	-7.99	34.09
MgReS <sub>2</sub>	164	-317.11	560.51	87.02	201.11	53.07	63.25	-438.81
MgFeS <sub>2</sub>	164	145.20	60.62	58.25	175.83	42.83	-4.76	42.29
MgRuS <sub>2</sub>	164	210.89	86.64	75.87	196.78	59.03	16.89	62.13
MgOsS <sub>2</sub>	164	229.74	84.45	69.45	226.69	53.15	16.65	72.64
MgCoS <sub>2</sub>	164	153.56	88.80	68.69	176.44	37.62	-19.12	32.38
MgRhS <sub>2</sub>	164	144.29	89.52	84.63	161.38	21.86	-7.73	27.39
MgIrS <sub>2</sub>	164	155.71	99.68	78.60	177.02	15.36	-11.90	28.01
MgNiS <sub>2</sub>	164	158.58	63.06	56.31	164.48	41.37	-3.67	47.76
MgPdS <sub>2</sub>	164	110.55	94.45	78.00	141.52	-14.39	-27.68	8.05
MgPtS <sub>2</sub>	164	101.15	110.08	82.00	149.54	-45.86	-44.74	-4.47
MgCuS <sub>2</sub>	164	118.70	75.91	63.51	149.17	2.37	-27.20	21.40
MgAgS <sub>2</sub>	164	94.62	77.82	61.23	116.03	-31.73	-29.70	8.40
MgAuS <sub>2</sub>	164	93.84	97.63	69.02	130.80	-89.68	-53.36	-1.90
MgGeS <sub>2</sub>	164	125.53	46.10	40.60	146.76	47.22	11.62	39.72
MgSnS <sub>2</sub>	164	104.13	41.80	41.69	139.92	39.04	13.71	31.16
MgPbS <sub>2</sub>	164	104.66	41.09	39.22	141.53	39.52	14.83	31.78

Table S XV: Elements of the elastic matrix for magnesium-intercalated TMDC sulfides.

MgMSe <sub>2</sub>	Space Group	c <sub>11</sub> (GPa)	c <sub>12</sub> (GPa)	c <sub>13</sub> (GPa)	c <sub>33</sub> (GPa)	c <sub>44</sub> (GPa)	c <sub>14</sub> (GPa)	c <sub>66</sub> (GPa)
MgScSe <sub>2</sub>	164	125.68	42.98	49.62	144.18	52.88	5.25	41.35
MgYSe <sub>2</sub>	164	116.05	40.81	49.17	127.48	50.34	10.05	37.62
MgTiSe <sub>2</sub>	164	119.44	47.00	65.64	134.95	60.49	5.03	36.22
MgZrSe <sub>2</sub>	164	134.51	45.86	71.11	139.82	61.52	5.02	44.32
MgHfSe <sub>2</sub>	164	142.36	47.26	72.78	132.26	57.93	4.14	47.55
MgVSe <sub>2</sub>	164	130.50	55.55	50.90	128.86	44.98	9.54	37.48
MgNbSe <sub>2</sub>	164	125.08	54.63	85.59	157.30	64.36	3.73	35.23
MgTaSe <sub>2</sub>	164	130.17	64.92	81.81	128.84	50.57	2.91	32.62
MgCrSe <sub>2</sub>	164	1847.69	1850.66	1712.65	-787.21	11.76	-25.76	-1.49
MgMoSe <sub>2</sub>	164	132.26	68.23	67.48	142.13	58.08	12.43	32.01
MgWSe <sub>2</sub>	164	124.47	72.14	62.54	162.29	55.48	13.41	26.17
MgMnSe <sub>2</sub>	164	92.92	25.36	177.97	797.31	28.51	-1.15	33.78
MgReSe <sub>2</sub>	164	110.17	130.64	59.05	165.85	49.12	14.73	-10.24
MgFeSe <sub>2</sub>	164	175.77	65.50	62.78	142.06	58.14	0.79	55.13
MgRuSe <sub>2</sub>	164	181.88	75.24	66.61	147.46	53.08	11.06	53.32
MgOsSe <sub>2</sub>	164	198.89	72.71	61.21	174.85	50.12	9.76	63.09
MgCoSe <sub>2</sub>	164	130.89	72.50	64.05	124.15	34.38	-14.76	29.20
MgRhSe <sub>2</sub>	164	135.02	80.96	72.63	120.06	30.85	-4.27	27.03
MgIrSe <sub>2</sub>	164	142.96	85.67	69.75	138.94	26.48	-10.06	28.64
MgNiSe <sub>2</sub>	164	120.28	57.18	56.18	126.61	30.06	-8.57	31.55
MgPdSe <sub>2</sub>	164	101.63	76.84	69.04	96.97	4.13	-14.66	12.39
MgPtSe <sub>2</sub>	164	96.76	86.00	70.11	113.19	-1.24	-22.54	5.38
MgCuSe <sub>2</sub>	164	99.43	66.47	63.18	94.86	-6.18	-21.99	16.48
MgAgSe <sub>2</sub>	164	83.31	62.49	57.92	89.07	-8.30	-14.36	10.41
MgAuSe <sub>2</sub>	164	86.06	74.40	63.98	93.51	-36.71	-26.68	5.83
MgGeSe <sub>2</sub>	164	108.55	40.32	37.44	119.97	42.00	10.11	34.11
MgSnSe <sub>2</sub>	164	90.91	37.94	36.97	112.33	35.50	11.59	26.49
MgPbSe <sub>2</sub>	164	89.28	36.55	35.35	114.03	35.10	12.56	26.36

Table S XVI: Elements of the elastic matrix for magnesium-intercalated TMDC selenides.

MgMTe <sub>2</sub>	Space Group	c <sub>11</sub> (GPa)	c <sub>12</sub> (GPa)	c <sub>13</sub> (GPa)	c <sub>33</sub> (GPa)	c <sub>44</sub> (GPa)	c <sub>14</sub> (GPa)	c <sub>66</sub> (GPa)
MgScTe <sub>2</sub>	164	91.70	37.69	41.11	96.43	41.09	4.18	27.01
MgYTe <sub>2</sub>	164	81.69	34.17	40.24	93.43	40.75	7.21	23.76
MgTiTe <sub>2</sub>	164	59.92	27.16	27.96	74.74	43.02	4.00	16.38
MgZrTe <sub>2</sub>	164	78.89	46.28	64.13	85.18	49.20	7.23	16.30
MgHfTe <sub>2</sub>	164	78.23	51.35	56.90	92.64	50.52	7.95	13.44
MgVTe <sub>2</sub>	164	104.92	46.21	42.11	85.40	37.11	6.99	29.35
MgNbTe <sub>2</sub>	164	89.10	53.11	66.79	93.15	53.01	6.23	17.99
MgTaTe <sub>2</sub>	164	-14.43	161.54	58.32	101.15	50.67	23.60	-87.99
MgCrTe <sub>2</sub>	164	85.56	46.39	42.76	98.51	22.21	-3.05	19.58
MgMoTe <sub>2</sub>	164	115.49	58.61	51.08	99.01	51.63	7.05	28.44
MgWTe <sub>2</sub>	164	117.94	62.97	51.65	115.42	52.16	6.90	27.48
MgMnTe <sub>2</sub>	164	117.78	69.44	39.38	8.97	40.15	-5.35	24.17
MgReTe <sub>2</sub>	164	134.66	68.74	55.09	126.40	51.26	-0.38	32.96
MgFeTe <sub>2</sub>	164	142.87	53.91	52.60	93.66	52.11	-7.14	44.48
MgRuTe <sub>2</sub>	164	154.23	62.42	54.19	104.59	50.76	2.06	45.91
MgOsTe <sub>2</sub>	164	179.15	61.20	53.09	127.16	53.68	0.71	58.97
MgCoTe <sub>2</sub>	164	111.58	51.83	55.52	81.37	34.18	-12.56	29.88
MgRhTe <sub>2</sub>	164	117.98	62.09	58.70	81.94	29.86	-9.19	27.94
MgIrTe <sub>2</sub>	164	128.15	70.76	60.31	98.80	27.49	-17.61	28.70
MgNiTe <sub>2</sub>	164	92.78	52.42	61.30	69.54	21.21	-13.76	20.18
MgPdTe <sub>2</sub>	164	94.28	59.79	55.91	70.36	15.31	-9.45	17.24
MgPtTe <sub>2</sub>	164	101.29	65.78	59.30	81.27	13.88	-15.32	17.75
MgCuTe <sub>2</sub>	164	76.76	48.79	53.23	65.53	-1.50	-15.73	13.98
MgAgTe <sub>2</sub>	164	65.16	47.76	47.54	62.86	-4.32	-10.43	8.70
MgAuTe <sub>2</sub>	164	71.59	55.64	56.01	58.87	-16.79	-16.98	7.98
MgGeTe <sub>2</sub>	164	84.53	29.12	29.92	87.90	36.26	8.17	27.71
MgSnTe <sub>2</sub>	164	74.15	30.59	30.41	84.61	31.66	9.25	21.78
MgPbTe <sub>2</sub>	164	71.11	29.51	29.84	84.67	30.15	10.21	20.80

Table S XVII: Elements of the elastic matrix for magnesium-intercalated TMDC tellurides.

### 1. Materials Project

The elastic properties of several of the materials that have been considered in this work have been presented on the Materials Project<sup>19</sup>. Where multiple phases of a material are available on the Materials Project, we have selected the structure that resembles the TMDC phase structure presented here for the most direct comparison. In general, we find good agreement with many of the values provided in the Materials Project, particularly for intercalated TMDCs. We also see close agreement with the  $c_{11}$ ,  $c_{12}$  and  $c_{66}$  elements of many of the pristine TMDCs, but significant differences are present for  $c_{13}$ ,  $c_{33}$ , and  $c_{44}$ . The Materials Project use the PBE functional in VASP with a plane-wave energy cutoff of 700 eV<sup>20</sup>, which is the same as we employ in this work. However, The Materials Project uses 7000 k-points per reciprocal atom (pra), whereas we use 17,496 pra in the pristine systems, and 23,328 pra in the intercalated systems. The difference in results is likely due to this as the elements of the elastic tensor can be sensitive to the sampling of reciprocal space<sup>18</sup>.

Material	Space Group	c <sub>11</sub> (GPa)	c <sub>12</sub> (GPa)	c <sub>13</sub> (GPa)	c <sub>33</sub> (GPa)	c <sub>44</sub> (GPa)	c <sub>14</sub> (GPa)	c <sub>66</sub> (GPa)	Source
TiS <sub>2</sub>	164	121	25	1	4	2	-1	48	MP-2156 <sup>45</sup>
TiS <sub>2</sub>	164	137.22	26.95	7.87	32.77	11.39	3.21	55.13	TW
LiTiS <sub>2</sub>	164	150	37	30	122	40	-3	57	MP-9615 <sup>46</sup>
LiTiS <sub>2</sub>	164	160.33	37.30	31.19	129.00	47.94	2.23	61.51	TW
TiSe <sub>2</sub>	164	93	20	3	5	2	-1	27	MP-2194 <sup>47</sup>
TiSe <sub>2</sub>	164	101.21	21.14	13.42	24.01	11.82	4.07	40.04	TW
TiTe <sub>2</sub>	164	70	19	9	10	8	-3	25	MP-1907 <sup>48</sup>
TiTe <sub>2</sub>	164	77.49	18.02	12.83	35.47	17.16	6.15	29.73	TW
LiTiTe <sub>2</sub>	164	71	16	27	60	29	-1	27	MP-10189 <sup>49</sup>
LiTiTe <sub>2</sub>	164	75.41	14.88	28.27	69.20	34.39	0.69	30.27	TW
ZrS <sub>2</sub>	164	122	22	1	4	1	0	45	MP-1186 <sup>50</sup>
ZrS <sub>2</sub>	164	134.21	26.51	7.65	34.19	8.57	2.43	53.85	TW
ZrSe <sub>2</sub>	164	95	20	2	8	2	-1	37	MP-2076 <sup>51</sup>
ZrSe <sub>2</sub>	164	108.49	22.15	6.70	32.62	9.50	2.65	43.17	TW
ZrTe <sub>2</sub>	164	61	10	3	12	7	-2	26	MP-1018107 <sup>52</sup>
ZrTe <sub>2</sub>	164	65.99	11.13	8.54	33.97	13.74	4.88	27.43	TW
HfTe <sub>2</sub>	164	62	9	2	14	5	-2	27	MP-32887 <sup>53</sup>
HfTe <sub>2</sub>	164	67.86	10.47	8.81	29.17	13.69	4.66	28.70	TW
LiVS <sub>2</sub>	164	84	92	33	110	36	-4	-4	MP-7543 <sup>54</sup>
LiVS <sub>2</sub>	164	166.11	30.06	49.75	129.97	57.89	0.09	68.02	TW
VSe <sub>2</sub>	164	99	14	3	5	1	-1	43	MP-694 <sup>55</sup>
VSe <sub>2</sub>	164	116.37	14.94	13.72	24.44	12.11	5.53	50.71	TW
NbS <sub>2</sub>	164	134	30	-3	4	2	-1	52	MP-995122 <sup>56</sup>
NbS <sub>2</sub>	164	163.34	30.73	9.74	39.70	9.87	7.54	66.31	TW
NbSe <sub>2</sub>	164	116	26	5	15	4	-2	45	MP-10228 <sup>57</sup>
NbSe <sub>2</sub>	164	140.09	25.64	10.55	39.59	18.53	7.05	57.22	TW
CrS <sub>2</sub>	164	113	36	16	17	9	2	39	MP-755263 <sup>58</sup>
CrS <sub>2</sub>	164	185.59	9.27	23.74	41.04	11.49	5.31	88.29	TW
CrTe <sub>2</sub>	164	68	23	18	32	9	4	23	MP-685055 <sup>59</sup>
CrTe <sub>2</sub>	164	1178.75	1090.03	416.76	167.31	12.41	-0.33	44.36	TW
SnS <sub>2</sub>	164	99	24	0	2	1	0	38	MP-1170 <sup>60</sup>
SnS <sub>2</sub>	164	120.30	31.13	10.07	25.27	7.88	0.79	44.58	TW
SnSe <sub>2</sub>	164	85	21	3	5	2	0	32	MP-665 <sup>61</sup>
SnSe <sub>2</sub>	164	97.63	26.17	12.36	23.25	7.68	0.98	35.73	TW

Table S XVIII: Elements of the elastic matrix for relevant materials presented on the Materials Project (MP). Values obtained in this work (TW) have also been included for comparison.

### C. Elastic Stability

In Table SXIX, we highlight the materials which break one or more of the elastic stability conditions, along with the conditions that are broken. The elastic stability conditions have been outlined elsewhere for different crystal systems<sup>62</sup>, which for trigonal crystals are,

$$\begin{aligned}
 (a) \quad & c_{11} > |c_{12}| \\
 (b) \quad & c_{44} > 0 \\
 (c) \quad & c_{13}^2 < \frac{1}{2}c_{33}(c_{11} + c_{12}) \\
 (d) \quad & c_{14}^2 < \frac{1}{2}c_{44}(c_{11} - c_{12}) = c_{44}c_{66}.
 \end{aligned} \tag{S5}$$

$\text{MX}_2$	Conditions	$\text{LiMX}_2$	Conditions	$\text{MgMX}_2$	Conditions
	Broken		Broken		Broken
$\text{ScS}_2$	b d	$\text{LiFeS}_2$	a d	$\text{MgCrS}_2$	c
$\text{YS}_2$	b d	$\text{LiCuS}_2$	d	$\text{MgMnS}_2$	a c
$\text{RuS}_2$	d	$\text{LiAgS}_2$	b d	$\text{MgPdS}_2$	b d
$\text{PbS}_2$	b d	$\text{LiAuS}_2$	a b d	$\text{MgPtS}_2$	a b d
$\text{ScSe}_2$	b d	$\text{LiMnSe}_2$	a b c d	$\text{MgCuS}_2$	d
$\text{YSe}_2$	b d	$\text{LiAuSe}_2$	b d	$\text{MgAgS}_2$	b d
$\text{FeSe}_2$	a c d	$\text{LiCrTe}_2$	c	$\text{MgAuS}_2$	a b d
$\text{RuSe}_2$	d	$\text{LiMnTe}_2$	c	$\text{MgCrSe}_2$	a c d
$\text{RhSe}_2$	d	$\text{LiReTe}_2$	a d	$\text{MgReSe}_2$	a d
$\text{PbSe}_2$	a b d	$\text{LiPbTe}_2$	a d	$\text{MgPdSe}_2$	d
$\text{YTe}_2$	b d			$\text{MgPtSe}_2$	b d
$\text{PdTe}_2$	a b d			$\text{MgCuSe}_2$	b d
				$\text{MgAgSe}_2$	b d
				$\text{MgAuSe}_2$	b d
				$\text{MgCrSe}_2$	a c d
				$\text{MgReSe}_2$	a d
				$\text{MgPdSe}_2$	d
				$\text{MgPtSe}_2$	b d
				$\text{MgCuSe}_2$	b d
				$\text{MgAgSe}_2$	b d
				$\text{MgAuSe}_2$	b d
				$\text{MgTaTe}_2$	a c d
				$\text{MgMnTe}_2$	c
				$\text{MgCuTe}_2$	b d
				$\text{MgAgTe}_2$	b d
				$\text{MgAuTe}_2$	b d

Table S XIX: Table indicated which materials are not elastically stable, and the stability conditions they break.

## D. Elastic Quantities

In the main article, we highlighted the elastic properties of the sulfide materials. Here, we present the equivalent data for the analogous selenide and telluride materials. The bulk and shear moduli are shown in Figure S3. The Hill values of bulk ( $B_{VRH}$ ) and shear ( $G_{VRH}$ ) moduli provide an intermediate to the Voigt upper limit and the Reuss lower limit. Many of the other elastic properties are derived from these values of bulk and shear moduli, and we only present those calculated from  $B_{VRH}$  and  $G_{VRH}$  in the main article for brevity and clarity of figures. In the following, we also include the values determined with the Voigt and Reuss schemes. Figure S4 presents the Young's modulus, and Figure S5 presents the elastic ratios indicating material ductility.

To supplement the graphical presentation of the elastic quantities (bulk, shear, and Young's moduli, along with the Poisson and Pugh ratios), we also include numerical values for convenience. This includes data for the pristine TMDCs (Table SXX, Table SXXI and Table SXXII), as well as the lithium-intercalated (Table SXXIII, Table SXXIV and Table SXXV) and magnesium-intercalated (Table SXXVI, Table SXXVII and Table SXXVIII) structures.

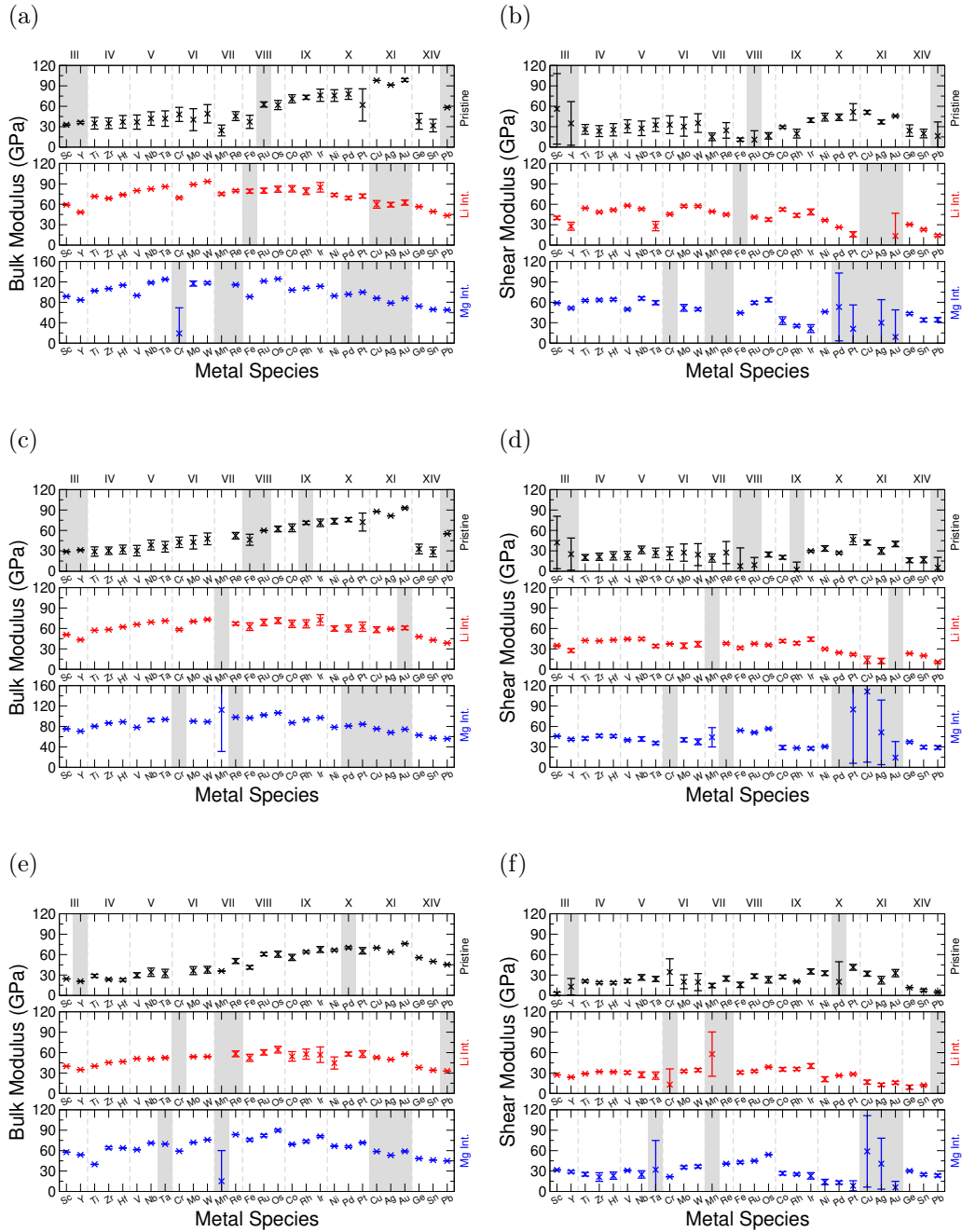


Figure S 3: Bulk modulus for sulfide (S3a), selenide (S3c), and telluride (S3e) TMDC materials. We similarly show the shear modulus for sulfide (S3b), selenide (S3d), and telluride (S3f) materials. Values calculated using the VRH scheme are presented with crosses, and the corresponding Reuss and Voigt results are presented as error bars. Data for the pristine bulk, lithium-intercalated, and magnesium-intercalated structures is presented in black, red, and blue, respectively. Materials which are not elastically stable are indicated with shaded regions.

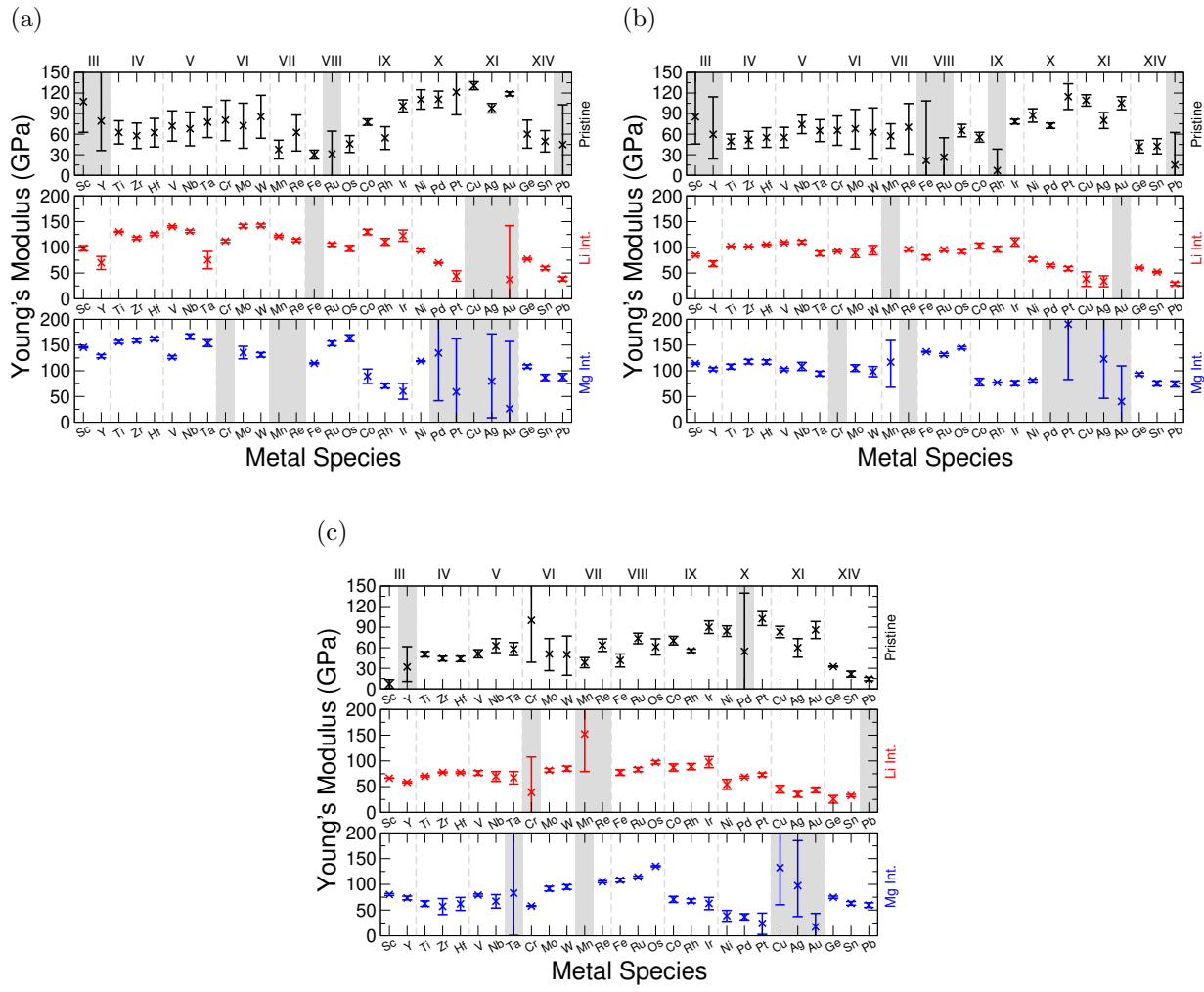


Figure S 4: Young's modulus for sulfide (S4a), selenide (S4b), and telluride (S4c) TMDC materials. Values calculated using the VRH scheme are presented with crosses, and the corresponding Reuss and Voigt results are presented as error bars. Data for the pristine bulk, lithium-intercalated, and magnesium-intercalated structures is presented in black, red, and blue, respectively. Materials which are not elastically stable are indicated with shaded regions.

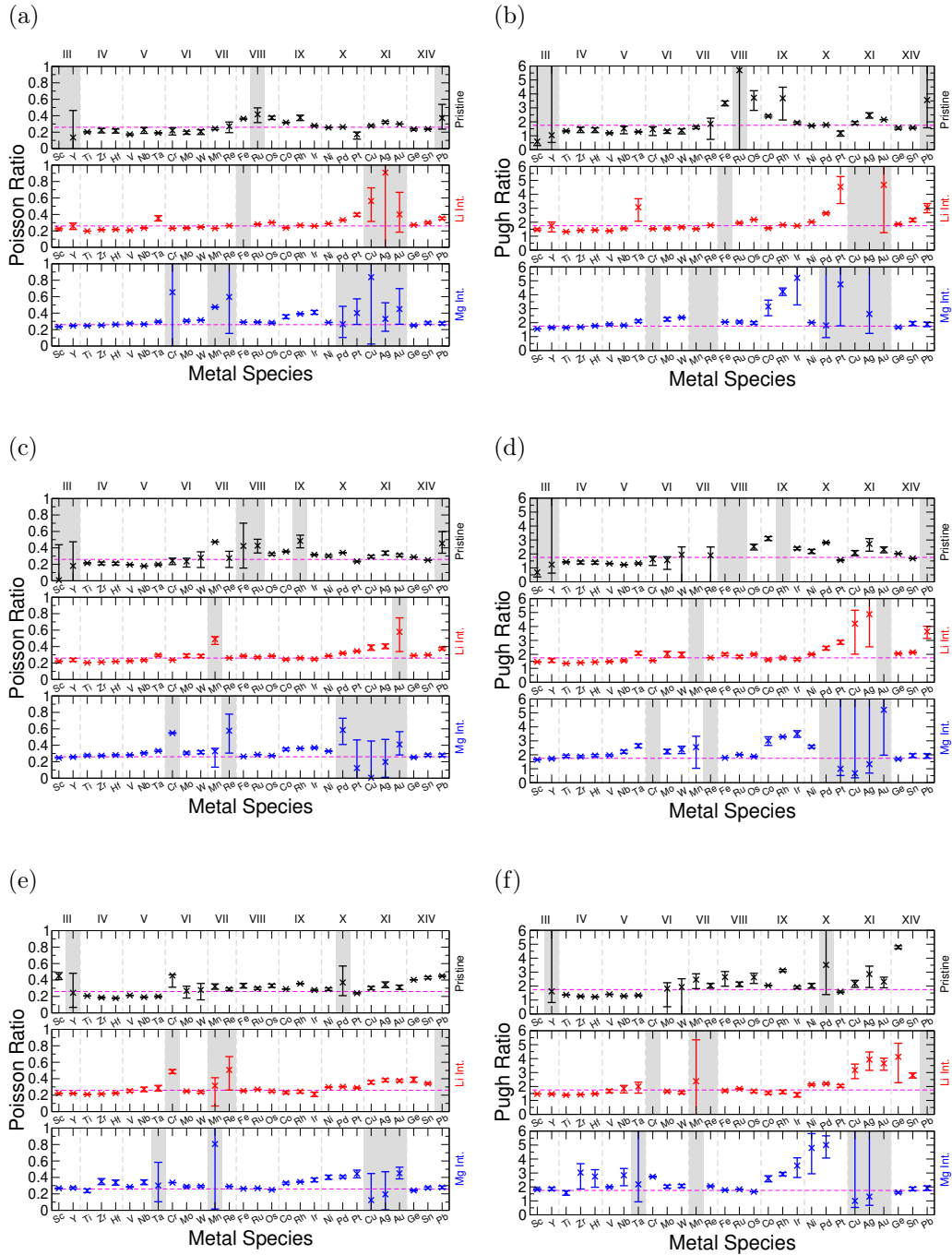


Figure S 5: Values of Poisson ratio for sulfides (S5a), selenides (S5c), and tellurides (S5e), and Pugh ratio for sulfides (S5b), selenides (S5d), and tellurides (S5f). Crosses indicate those calculated using the VRH scheme, and the corresponding Reuss and Voigt results are presented as error bars. Data for the pristine bulk, lithium-intercalated, and magnesium-intercalated structures is presented in black, red, and blue, respectively. A Poisson ratio of 0.26 and a Pugh ratio of 1.75 are indicated with horizontal dashed lines. Materials which are not elastically stable are indicated with shaded regions.

MX <sub>2</sub>	Bulk Modulus (GPa)			Shear Modulus (GPa)			Young's Modulus (GPa)			Poisson Ratio			Pugh Ratio		
	V	R	H	V	R	H	V	R	H	V	R	H	V	R	H
ScS <sub>2</sub>	33.91	31.94	32.92	4.39	107.99	56.19	12.63	152.30	107.44	0.44	-0.29	-0.04	7.72	0.30	0.59
YS <sub>2</sub>	37.71	34.66	36.18	2.78	66.91	34.85	8.15	122.14	79.13	0.46	-0.09	0.14	13.55	0.52	1.04
TiS <sub>2</sub>	43.62	26.51	35.07	33.22	18.85	26.03	79.48	45.72	62.61	0.20	0.21	0.20	1.31	1.41	1.35
ZrS <sub>2</sub>	42.92	27.10	35.01	31.59	15.53	23.56	76.09	39.12	57.73	0.20	0.26	0.23	1.36	1.74	1.49
HfS <sub>2</sub>	46.43	27.76	37.10	34.49	16.49	25.49	82.93	41.30	62.22	0.20	0.25	0.22	1.35	1.68	1.46
VS <sub>2</sub>	47.20	26.33	36.76	40.24	21.04	30.64	94.00	49.85	71.93	0.17	0.18	0.17	1.17	1.25	1.20
NbS <sub>2</sub>	51.87	32.05	41.96	38.29	16.86	27.57	92.18	43.04	67.86	0.20	0.28	0.23	1.35	1.90	1.52
TaS <sub>2</sub>	53.24	30.52	41.88	42.19	22.98	32.58	100.11	55.10	77.62	0.19	0.20	0.19	1.26	1.33	1.29
CrS <sub>2</sub>	58.44	37.73	48.09	46.02	19.79	32.90	109.35	50.54	80.38	0.19	0.28	0.22	1.27	1.91	1.46
MoS <sub>2</sub>	56.43	24.19	40.31	44.17	16.06	30.12	105.10	39.45	72.33	0.19	0.23	0.20	1.28	1.51	1.34
WS <sub>2</sub>	62.49	35.55	49.02	49.08	21.66	35.37	116.69	54.02	85.54	0.19	0.25	0.21	1.27	1.64	1.39
MnS <sub>2</sub>	32.42	16.48	24.45	20.68	9.50	15.09	51.15	23.90	37.54	0.24	0.26	0.24	1.57	1.74	1.62
ReS <sub>2</sub>	52.12	39.06	45.59	36.03	13.16	24.60	87.85	35.50	62.54	0.22	0.35	0.27	1.44	2.97	1.85
FeS <sub>2</sub>	46.79	27.46	37.14	13.40	8.74	11.07	36.70	23.72	30.21	0.37	0.36	0.36	3.49	3.14	3.35
RuS <sub>2</sub>	66.50	58.78	62.64	24.03	-2.05	10.99	64.35	-6.23	31.15	0.34	0.52	0.42	2.77	-28.64	5.70
OsS <sub>2</sub>	68.57	55.11	61.84	21.31	11.91	16.61	57.94	33.33	45.74	0.36	0.40	0.38	3.22	4.63	3.72
CoS <sub>2</sub>	76.87	65.05	70.96	31.08	27.77	29.43	82.17	72.94	77.56	0.32	0.31	0.32	2.47	2.34	2.41
RhS <sub>2</sub>	76.14	70.23	73.19	13.39	19.85	70.77	37.76	54.60	0.35	0.41	0.38	2.89	5.25	3.69	
IrS <sub>2</sub>	85.22	67.26	76.24	42.79	36.33	39.56	109.97	92.36	101.18	0.28	0.27	0.28	1.99	1.85	1.93
NiS <sub>2</sub>	84.40	67.17	75.79	49.79	38.25	44.02	124.82	96.43	110.63	0.25	0.26	0.26	1.70	1.76	1.72
PdS <sub>2</sub>	85.76	70.20	77.98	48.64	39.08	43.86	122.72	98.90	110.81	0.26	0.27	0.26	1.76	1.80	1.78
PtS <sub>2</sub>	85.63	38.21	61.92	63.88	39.49	51.69	153.47	88.12	121.31	0.20	0.12	0.17	1.34	0.97	1.20
CuS <sub>2</sub>	97.85	97.85	97.85	48.49	53.85	51.17	136.51	124.85	130.73	0.27	0.29	0.28	1.82	2.03	1.91
AgS <sub>2</sub>	91.50	91.21	91.36	39.94	34.08	37.02	104.59	90.92	97.82	0.31	0.33	0.32	2.29	2.68	2.47
AuS <sub>2</sub>	100.78	96.47	98.62	46.89	44.58	45.74	121.78	115.89	118.84	0.30	0.30	0.30	2.15	2.16	2.16
GeS <sub>2</sub>	49.62	26.35	37.98	32.69	15.85	24.27	80.42	39.62	60.03	0.23	0.25	0.24	1.53	1.66	1.56
SnS <sub>2</sub>	40.93	22.41	31.67	26.38	13.63	20.00	65.14	33.99	49.57	0.23	0.25	0.24	1.55	1.64	1.58
PbS <sub>2</sub>	58.22	58.07	58.14	-4.31	36.98	16.33	-13.27	91.50	44.80	0.54	0.24	0.37	-13.50	1.57	3.56

Table S XX: Elastic moduli and ratios for pristine TMDC sulfides.

MX <sub>2</sub>	Bulk Modulus (GPa)			Shear Modulus (GPa)			Young's Modulus (GPa)			Poisson Ratio			Pugh Ratio		
	V	R	H	V	R	H	V	R	H	V	R	H	V	R	H
ScSe <sub>2</sub>	29.08	28.52	28.80	3.76	80.81	42.28	10.81	124.67	85.17	0.44	-0.23	0.01	7.74	0.35	0.68
YSe <sub>2</sub>	31.87	30.45	31.16	1.69	48.86	25.27	4.96	95.50	59.68	0.47	-0.02	0.18	18.93	0.62	1.23
TiSe <sub>2</sub>	35.82	22.08	28.95	24.63	16.10	20.36	60.11	38.85	49.49	0.22	0.21	0.22	1.45	1.37	1.42
ZrSe <sub>2</sub>	35.63	24.68	30.16	26.70	15.99	21.35	64.10	39.45	51.82	0.20	0.23	0.21	1.33	1.54	1.41
HfSe <sub>2</sub>	38.45	25.33	31.89	28.92	16.54	22.73	69.37	40.75	55.10	0.20	0.23	0.21	1.33	1.53	1.40
VSe <sub>2</sub>	37.99	22.60	30.30	29.30	16.90	23.10	69.93	40.58	55.26	0.19	0.20	0.20	1.30	1.34	1.31
NbSe <sub>2</sub>	45.92	31.27	38.60	37.06	25.86	31.46	87.61	60.81	74.21	0.18	0.18	0.18	1.24	1.21	1.23
TaSe <sub>2</sub>	43.85	28.21	36.03	34.01	20.34	27.17	81.08	49.19	65.15	0.19	0.21	0.20	1.29	1.39	1.33
CrSe <sub>2</sub>	50.25	34.98	42.62	35.64	16.96	26.30	86.48	43.81	65.45	0.21	0.29	0.24	1.41	2.06	1.62
MoSe <sub>2</sub>	52.62	32.77	42.70	40.16	14.81	27.48	96.05	38.60	67.88	0.20	0.30	0.24	1.31	2.21	1.55
WSe <sub>2</sub>	56.26	39.02	47.64	40.63	8.38	24.51	98.25	23.45	62.76	0.21	0.40	0.28	1.38	4.66	1.94
MnSe <sub>2</sub>	222.96	455.63	339.30	13.45	25.49	19.47	39.55	75.07	57.31	0.47	0.47	0.47	16.58	17.87	17.43
ReSe <sub>2</sub>	57.03	47.44	52.23	43.78	11.16	27.47	104.58	31.05	70.12	0.19	0.39	0.28	1.30	4.25	1.90
FeSe <sub>2</sub>	54.37	38.25	46.31	-19.23	34.37	7.57	-65.40	79.34	21.53	0.70	0.15	0.42	-2.83	1.11	6.12
RuSe <sub>2</sub>	60.37	59.51	59.94	20.30	-1.83	9.24	54.76	-5.55	26.35	0.35	0.52	0.43	2.97	-32.52	6.49
OsSe <sub>2</sub>	66.39	57.97	62.18	28.30	20.98	24.64	74.34	56.16	65.29	0.31	0.34	0.32	2.35	2.76	2.52
CoSe <sub>2</sub>	69.56	58.08	63.82	23.19	17.73	20.46	62.62	48.27	55.46	0.35	0.36	0.36	3.00	3.28	3.12
RhSe <sub>2</sub>	73.50	68.91	71.21	13.49	-8.86	2.31	38.14	-27.78	6.87	0.41	0.57	0.48	5.45	-7.77	30.78
IrSe <sub>2</sub>	76.72	65.71	71.22	30.90	28.54	29.72	81.73	74.80	78.28	0.32	0.31	0.32	2.48	2.30	2.40
NiSe <sub>2</sub>	77.68	69.41	73.54	37.57	29.42	33.50	97.07	77.34	87.25	0.29	0.31	0.30	2.07	2.36	2.20
PdSe <sub>2</sub>	78.77	72.91	75.84	28.46	25.48	26.97	76.20	68.46	72.33	0.34	0.34	0.34	2.77	2.86	2.81
PtSe <sub>2</sub>	85.52	59.08	72.30	53.86	39.02	46.44	133.55	95.93	114.75	0.24	0.23	0.24	1.59	1.51	1.56
CuSe <sub>2</sub>	87.80	87.78	87.79	46.01	38.58	42.29	117.51	100.92	109.32	0.28	0.31	0.29	1.91	2.2	2.076
AgSe <sub>2</sub>	81.64	81.28	81.46	34.83	25.05	29.94	91.48	68.16	80.02	0.31	0.36	0.34	2.34	3.24	2.72
AuSe <sub>2</sub>	93.92	91.76	92.84	44.19	36.06	40.12	114.59	95.64	105.21	0.30	0.33	0.31	2.13	2.54	2.31
GeSe <sub>2</sub>	39.93	25.59	32.76	19.80	12.66	16.23	50.97	32.61	41.79	0.29	0.29	0.29	2.02	2.02	2.02
SnSe <sub>2</sub>	35.59	21.29	28.44	21.39	12.49	16.94	53.47	31.34	42.40	0.25	0.25	0.25	1.66	1.70	1.68
PbSe <sub>2</sub>	55.05	55.05	55.05	-10.08	20.44	5.17	-32.23	54.56	15.05	0.60	0.33	0.45	-5.46	2.69	10.64

Table S XXI: Elastic moduli and ratios for pristine TMDC selenides.

MX <sub>2</sub>	Bulk Modulus (GPa)			Shear Modulus (GPa)			Young's Modulus (GPa)			Poisson Ratio			Pugh Ratio		
	V	R	H	V	R	H	V	R	H	V	R	H	V	R	H
ScTe <sub>2</sub>	24.35	24.32	24.34	4.74	0.35	2.55	13.37	1.05	7.39	0.40	0.49	0.45	5.13	69.20	9.55
YTe <sub>2</sub>	21.16	20.46	20.81	0.78	24.88	12.83	2.31	53.11	31.92	0.48	0.07	0.24	27.17	0.82	1.62
TiTe <sub>2</sub>	30.87	26.57	28.72	22.60	19.30	20.95	54.49	46.61	50.55	0.21	0.21	0.21	1.37	1.38	1.37
ZrTe <sub>2</sub>	24.71	22.31	23.51	20.16	17.05	18.61	47.55	40.77	44.17	0.18	0.20	0.19	1.23	1.31	1.26
HfTe <sub>2</sub>	24.56	20.99	22.78	20.34	16.80	18.57	47.81	39.79	43.80	0.18	0.18	0.18	1.21	1.25	1.23
VTe <sub>2</sub>	33.42	25.99	29.71	23.49	18.71	21.10	57.10	45.26	51.18	0.22	0.21	0.21	1.42	1.39	1.41
NbTe <sub>2</sub>	40.15	27.96	34.06	30.65	22.31	26.48	73.30	52.87	63.09	0.20	0.18	0.19	1.31	1.25	1.29
TaTe <sub>2</sub>	38.43	26.24	32.34	28.01	20.42	24.21	67.60	48.64	58.13	0.21	0.19	0.20	1.37	1.29	1.34
CrTe <sub>2</sub>	707.99	34.40	371.19	53.92	14.78	34.35	157.75	38.79	99.97	0.46	0.31	0.46	13.13	2.33	10.81
MoTe <sub>2</sub>	42.37	30.61	36.49	30.31	9.81	20.06	73.42	26.60	50.86	0.21	0.36	0.27	1.40	3.12	1.82
WTe <sub>2</sub>	42.80	32.75	37.77	32.11	7.07	19.59	77.06	19.79	50.11	0.20	0.40	0.28	1.33	4.63	1.93
MnTe <sub>2</sub>	36.16	35.45	35.81	17.67	11.39	14.53	45.60	30.86	38.40	0.29	0.35	0.32	2.05	3.11	2.46
ReTe <sub>2</sub>	54.27	46.83	50.55	28.57	20.91	24.74	72.91	54.59	63.80	0.28	0.31	0.29	1.90	2.24	2.04
FeTe <sub>2</sub>	43.91	38.68	41.29	19.49	11.70	15.60	50.94	31.89	41.56	0.31	0.36	0.33	2.25	3.31	2.65
RuTe <sub>2</sub>	63.10	58.40	60.75	31.60	25.10	28.35	81.25	65.87	73.61	0.29	0.31	0.30	2.00	2.33	2.14
OsTe <sub>2</sub>	65.14	56.11	60.62	27.83	18.23	23.03	73.08	49.35	61.33	0.31	0.35	0.33	2.34	3.08	2.63
CoTe <sub>2</sub>	60.37	51.32	55.84	29.75	24.84	27.30	76.66	64.17	70.42	0.29	0.29	0.29	2.03	2.07	2.05
RhTe <sub>2</sub>	65.36	62.46	63.91	21.45	19.54	20.49	58.00	53.08	55.54	0.35	0.36	0.36	3.05	3.20	3.12
IrTe <sub>2</sub>	71.94	63.10	67.52	39.01	31.38	35.20	99.11	80.76	89.96	0.27	0.29	0.28	1.84	2.01	1.92
NiTe <sub>2</sub>	67.87	65.21	66.54	36.08	29.33	32.70	91.94	76.52	84.30	0.27	0.30	0.29	1.88	2.22	2.03
PdTe <sub>2</sub>	71.62	68.85	70.23	-9.63	49.55	19.96	-30.24	119.88	54.69	0.57	0.21	0.37	-7.44	1.39	3.52
PtTe <sub>2</sub>	70.38	60.95	65.66	37.01	41.33	112.61	92.35	102.50	0.23	0.25	0.24	1.54	1.65	1.59	
CuTe <sub>2</sub>	70.01	69.84	69.93	35.59	28.27	31.93	91.30	74.74	83.14	0.29	0.32	0.30	1.97	2.47	2.19
AgTe <sub>2</sub>	63.94	63.87	63.91	28.00	16.75	22.37	73.29	46.21	60.11	0.31	0.38	0.34	2.28	3.81	2.86
AuTe <sub>2</sub>	76.45	75.73	76.09	38.19	27.43	32.81	98.21	73.43	86.06	0.29	0.34	0.31	2.00	2.76	2.32
GeTe <sub>2</sub>	55.82	55.24	55.53	11.89	11.29	11.59	33.32	31.72	32.52	0.40	0.40	0.40	4.69	4.89	4.79
SnTe <sub>2</sub>	50.06	49.96	50.01	9.13	5.95	7.54	25.83	17.18	21.55	0.41	0.44	0.43	5.48	8.39	6.63
PbTe <sub>2</sub>	45.95	44.78	45.36	5.78	4.05	4.92	16.65	11.79	14.23	0.44	0.46	0.45	7.95	11.06	9.23

Table S XXII: Elastic moduli and ratios for pristine TMDC tellurides.

LiMX <sub>2</sub>	Bulk Modulus (GPa)			Shear Modulus (GPa)			Young's Modulus (GPa)			Poisson Ratio			Pugh Ratio		
	V	R	H	V	R	H	V	R	H	V	R	H	V	R	H
LiScS <sub>2</sub>	60.22	58.29	59.26	42.46	37.78	40.12	93.21	98.20	0.21	0.23	0.22	1.42	1.54	1.48	
LiYS <sub>2</sub>	49.14	47.42	48.28	33.67	21.85	27.76	82.22	56.82	0.22	0.30	0.26	1.46	2.17	1.74	
LiTiS <sub>2</sub>	72.11	71.17	71.64	54.81	53.92	54.36	131.19	129.14	0.20	0.20	0.20	1.32	1.32	1.32	
LiZrS <sub>2</sub>	69.47	67.87	68.67	49.66	47.31	48.49	120.32	115.17	0.21	0.22	0.21	1.40	1.43	1.42	
LiHfS <sub>2</sub>	74.86	73.15	74.01	52.78	50.48	51.63	128.22	123.11	0.21	0.22	0.22	1.42	1.45	1.43	
LiVS <sub>2</sub>	80.15	79.91	80.03	58.93	57.24	58.08	142.00	138.61	0.20	0.21	0.21	1.36	1.40	1.38	
LiNbS <sub>2</sub>	82.64	82.60	82.62	54.28	51.87	53.08	133.59	128.68	0.23	0.24	0.24	1.52	1.59	1.56	
LiTaS <sub>2</sub>	85.93	85.86	85.89	34.80	21.04	27.92	91.99	58.36	0.32	0.39	0.35	2.47	4.08	3.08	
LiCrS <sub>2</sub>	70.77	68.30	69.54	46.63	44.34	45.48	114.70	109.35	0.23	0.23	0.23	1.52	1.54	1.53	
LiMoS <sub>2</sub>	89.16	88.97	89.07	58.84	55.68	57.26	144.68	138.21	0.23	0.24	0.24	1.52	1.60	1.56	
LiWS <sub>2</sub>	93.58	93.51	93.54	58.55	55.84	57.20	145.34	139.71	0.24	0.25	0.25	1.60	1.67	1.64	
LiMnS <sub>2</sub>	76.86	73.57	75.22	50.04	48.63	49.34	123.36	119.55	0.23	0.23	0.23	1.54	1.51	1.52	
LiReS <sub>2</sub>	81.27	78.41	79.84	46.11	43.74	44.92	116.32	110.64	0.26	0.26	0.26	1.76	1.79	1.78	
LiFeS <sub>2</sub>	82.13	76.40	79.27	16.61	-773.09	-378.24	46.69	977.37	1921.37	0.41	-1.63	-3.54	4.94	-0.10	-0.21
LiRuS <sub>2</sub>	83.89	76.39	80.14	42.20	39.93	41.07	108.43	102.01	0.28	0.28	0.28	1.99	1.91	1.95	
LiOsS <sub>2</sub>	86.71	77.73	82.22	39.81	35.38	37.59	103.57	92.16	0.30	0.30	0.30	2.18	2.20	2.19	
LiCoS <sub>2</sub>	87.45	78.07	82.76	54.46	50.53	52.50	135.29	124.69	0.24	0.23	0.24	1.61	1.55	1.58	
LiRhS <sub>2</sub>	84.04	74.31	79.18	46.32	41.11	43.71	117.39	104.13	0.27	0.27	0.27	1.81	1.81	1.81	
LiIrS <sub>2</sub>	91.97	77.97	84.97	53.12	44.37	48.74	133.63	111.88	0.26	0.26	0.26	1.73	1.76	1.74	
LiNiS <sub>2</sub>	75.68	71.77	73.72	37.53	35.47	36.50	96.61	91.37	0.29	0.29	0.29	2.02	2.02	2.02	
LiPdS <sub>2</sub>	71.43	67.02	69.22	26.53	25.93	26.23	70.82	68.91	0.33	0.33	0.33	2.69	2.58	2.64	
LiPtS <sub>2</sub>	74.96	69.15	72.05	19.70	12.06	15.88	54.35	34.20	0.38	0.42	0.40	3.80	5.73	4.54	
LiCuS <sub>2</sub>	65.49	54.37	59.93	13.51	-28.13	-7.31	37.93	-101.97	0.40	0.81	0.56	4.85	-1.93	-8.20	
LiAgS <sub>2</sub>	62.83	56.05	59.44	10.40	-86.70	-38.15	29.57	-536.91	-145.59	0.42	2.10	0.91	6.04	-0.65	-1.56
LiAuS <sub>2</sub>	66.35	58.72	62.53	-20.16	46.89	13.37	-67.30	111.10	37.43	0.67	0.18	0.40	-3.29	1.25	4.68
LiGeS <sub>2</sub>	56.89	56.09	56.49	31.00	29.63	30.31	78.70	75.57	77.14	0.27	0.28	0.27	1.84	1.89	1.86
LiSnS <sub>2</sub>	49.67	49.04	49.35	24.22	21.51	22.87	62.50	56.30	59.42	0.31	0.30	0.30	2.05	2.28	2.16
LiPbS <sub>2</sub>	43.59	43.26	43.42	15.83	12.67	14.25	42.36	34.62	38.53	0.34	0.37	0.35	2.75	3.42	3.05

Table S XXIII: Elastic moduli and ratios for lithium-intercalated TMDC sulfides.

LiMX <sub>2</sub>	Bulk Modulus (GPa)			Shear Modulus (GPa)			Young's Modulus (GPa)			Poisson Ratio			Pugh Ratio		
	V	R	H	V	R	H	V	R	H	V	R	H	V	R	H
LiScSe <sub>2</sub>	51.46	50.20	50.83	35.74	33.80	34.77	87.06	82.81	84.93	0.22	0.23	0.22	1.44	1.49	1.46
LiYSe <sub>2</sub>	43.85	42.78	43.31	30.20	24.94	27.57	73.67	62.64	68.22	0.22	0.26	0.24	1.45	1.72	1.57
LiTiSe <sub>2</sub>	57.30	57.16	57.23	42.44	42.12	42.28	102.10	101.45	101.78	0.20	0.20	0.20	1.35	1.36	1.35
LiZnSe <sub>2</sub>	58.67	58.00	58.33	42.09	41.37	41.73	101.91	100.27	101.09	0.21	0.21	0.21	1.39	1.40	1.40
LiHfSe <sub>2</sub>	62.71	61.73	62.22	43.54	42.64	43.09	106.08	103.98	105.03	0.22	0.22	0.22	1.44	1.45	1.44
LiVSe <sub>2</sub>	65.87	65.83	65.85	45.37	43.47	44.42	110.69	106.88	108.79	0.22	0.23	0.22	1.45	1.51	1.48
LiNbSe <sub>2</sub>	69.26	69.24	69.25	46.29	42.94	44.62	113.58	106.75	110.19	0.23	0.24	0.23	1.50	1.61	1.55
LiTaSe <sub>2</sub>	71.21	71.14	71.18	36.19	31.96	34.07	92.84	83.39	88.15	0.28	0.30	0.29	1.97	2.23	2.09
LiCrSe <sub>2</sub>	59.59	57.18	58.39	38.09	36.77	37.43	94.20	90.84	92.52	0.24	0.24	0.24	1.56	1.56	1.56
LiMoSe <sub>2</sub>	70.93	69.69	70.32	38.57	30.60	34.59	97.96	80.08	89.15	0.27	0.31	0.29	1.84	2.28	2.03
LiWSe <sub>2</sub>	74.14	72.23	73.18	40.82	32.81	36.82	103.48	85.48	94.59	0.27	0.30	0.28	1.82	2.20	1.99
LiMnSe <sub>2</sub>	-1105.30	540.13	-282.59	-95.39	83.86	-5.76	-278.16	239.21	-17.17	0.46	0.43	0.49	11.60	6.44	49.05
LiRbSe <sub>2</sub>	69.09	64.94	67.01	39.22	36.79	38.01	98.94	92.84	95.89	0.26	0.26	0.26	1.76	1.77	1.76
LiFeSe <sub>2</sub>	68.36	57.01	62.68	32.89	29.72	31.30	85.03	75.97	80.51	0.29	0.28	0.29	2.08	1.92	2.00
LiRuSe <sub>2</sub>	73.70	63.99	68.85	38.43	36.69	37.56	98.21	92.40	95.33	0.28	0.26	0.27	1.92	1.74	1.83
LiOsSe <sub>2</sub>	75.73	67.17	71.45	36.84	34.48	35.66	95.11	88.32	91.72	0.29	0.28	0.29	2.06	1.95	2.00
LiCoSe <sub>2</sub>	72.24	61.37	66.80	43.31	39.53	41.42	108.29	97.63	102.98	0.25	0.23	0.24	1.67	1.55	1.61
LiRhSe <sub>2</sub>	72.79	60.86	66.83	40.35	36.29	38.32	102.17	90.82	96.51	0.27	0.25	0.26	1.80	1.68	1.74
LilrSe <sub>2</sub>	80.27	64.68	72.48	47.12	41.23	44.18	118.23	102.01	110.15	0.25	0.24	0.25	1.70	1.57	1.64
LiNiSe <sub>2</sub>	63.79	55.96	59.87	31.18	28.51	29.84	80.43	73.11	76.77	0.29	0.28	0.29	2.05	1.96	2.01
LiPdSe <sub>2</sub>	64.99	54.95	59.97	25.31	23.73	24.52	67.21	62.23	64.74	0.33	0.31	0.32	2.57	2.32	2.45
LiPtSe <sub>2</sub>	69.44	55.70	62.57	23.15	20.44	21.79	62.50	54.63	58.57	0.35	0.34	0.34	3.00	2.73	2.87
LiCuSe <sub>2</sub>	62.46	53.86	58.16	19.24	8.42	13.83	52.35	24.02	38.45	0.36	0.43	0.39	3.25	6.39	4.20
LiAgSe <sub>2</sub>	60.15	58.39	59.28	16.21	8.10	12.16	44.63	23.22	34.13	0.38	0.43	0.40	3.71	7.21	4.88
LiAuSe <sub>2</sub>	63.30	58.34	60.82	12.46	-30.61	-9.07	35.08	-111.30	-28.65	0.41	0.82	0.58	5.08	-1.91	-6.70
LiGeSe <sub>2</sub>	48.18	47.51	47.84	23.88	22.67	23.27	61.48	58.67	60.08	0.29	0.29	0.29	2.02	2.10	2.06
LiSnSe <sub>2</sub>	43.28	42.56	42.92	20.62	19.41	20.01	53.37	50.55	51.97	0.29	0.30	0.30	2.10	2.19	2.14
LiPbSe <sub>2</sub>	38.69	38.41	38.55	11.90	9.32	10.61	32.38	25.86	29.15	0.36	0.39	0.37	3.25	4.12	3.63

Table S XXIV: Elastic moduli and ratios for lithium-intercalated TMDC selenides.

LiMX <sub>2</sub>	Bulk Modulus (GPa)			Shear Modulus (GPa)			Young's Modulus (GPa)			Poisson Ratio			Pugh Ratio		
	V	R	H	V	R	H	V	R	H	V	R	H	V	R	H
LiScTe <sub>2</sub>	40.20	39.64	39.92	27.37	27.08	27.22	66.92	66.17	66.54	0.22	0.22	0.22	1.47	1.46	1.47
LiYTe <sub>2</sub>	35.13	34.73	34.93	24.55	23.32	23.94	59.74	57.17	58.46	0.22	0.23	0.22	1.43	1.49	1.46
LiTiTe <sub>2</sub>	40.32	40.22	40.27	29.71	28.36	29.04	71.56	68.88	70.23	0.20	0.21	0.21	1.36	1.42	1.39
LiZrTe <sub>2</sub>	45.41	45.21	45.31	32.44	31.45	31.95	78.61	76.60	77.60	0.21	0.22	0.21	1.40	1.44	1.42
LiHfTe <sub>2</sub>	46.81	46.50	46.65	32.36	30.72	31.54	78.90	75.52	77.22	0.22	0.23	0.22	1.45	1.51	1.48
LiVTe <sub>2</sub>	51.49	50.97	51.23	32.74	28.52	30.63	81.04	72.11	76.62	0.24	0.26	0.25	1.57	1.79	1.67
LiNbTe <sub>2</sub>	51.56	50.08	50.82	31.78	23.19	27.49	79.10	60.26	69.86	0.24	0.30	0.27	1.62	2.16	1.85
LiTaTe <sub>2</sub>	53.34	51.49	52.42	31.61	20.80	26.21	79.18	55.00	67.39	0.25	0.32	0.29	1.69	2.48	2.00
LiCrTe <sub>2</sub>	449.87	481.73	465.80	-10.01	36.06	13.03	-30.24	105.53	38.71	0.51	0.46	0.49	-44.96	13.36	35.76
LiMoTe <sub>2</sub>	54.67	53.17	53.92	34.35	31.11	32.73	85.20	78.11	81.67	0.24	0.26	0.25	1.59	1.71	1.65
LiWTe <sub>2</sub>	54.72	53.40	54.06	36.59	32.04	34.32	89.76	80.10	84.97	0.23	0.25	0.24	1.50	1.67	1.58
LiMnTe <sub>2</sub>	483.05	-207.84	137.61	90.30	25.32	57.81	255.01	79.19	152.13	0.41	0.56	0.32	5.35	-8.21	2.38
LiReTe <sub>2</sub>	62.52	53.93	58.22	21.62	-23.22	-0.80	58.16	-81.32	-2.41	0.34	0.75	0.51	2.89	-2.32	-72.93
LiFeTe <sub>2</sub>	57.56	47.12	52.34	32.81	28.95	30.88	82.71	72.08	77.41	0.26	0.25	0.25	1.75	1.63	1.70
LiRuTe <sub>2</sub>	64.17	56.39	60.28	34.25	31.25	32.75	87.24	79.13	83.19	0.27	0.27	0.27	1.87	1.80	1.84
LiOsTe <sub>2</sub>	69.29	59.40	64.34	39.88	37.93	38.91	100.39	93.82	97.14	0.26	0.24	0.25	1.74	1.57	1.65
LiCoTe <sub>2</sub>	61.47	47.44	54.45	37.85	32.94	35.39	94.21	80.24	87.27	0.24	0.22	0.23	1.62	1.44	1.54
LiRhTe <sub>2</sub>	65.24	50.39	57.81	37.77	33.80	35.78	94.97	82.88	88.99	0.26	0.23	0.24	1.73	1.49	1.62
LiIrTe <sub>2</sub>	68.32	45.53	56.92	43.85	36.74	40.30	108.37	86.86	97.81	0.24	0.18	0.21	1.56	1.24	1.41
LiNiTe <sub>2</sub>	53.62	35.83	44.73	24.55	17.26	20.90	63.89	44.61	54.26	0.30	0.29	0.30	2.18	2.08	2.14
LiPdTe <sub>2</sub>	60.73	55.09	57.91	26.98	25.69	26.33	70.49	66.70	68.60	0.31	0.30	0.30	2.25	2.14	2.20
LiPtTe <sub>2</sub>	62.94	52.89	57.92	29.54	27.18	28.36	76.63	69.62	73.15	0.30	0.28	0.29	2.13	1.95	2.04
LiCuTe <sub>2</sub>	53.90	51.74	52.82	19.61	13.66	16.63	52.46	37.66	45.16	0.34	0.38	0.36	2.75	3.79	3.18
LiAgTe <sub>2</sub>	50.22	49.56	49.89	14.85	10.55	12.70	40.56	29.54	35.12	0.37	0.40	0.38	3.38	4.70	3.93
LiAuTe <sub>2</sub>	58.51	57.26	57.89	17.86	13.83	15.84	48.62	38.39	43.55	0.36	0.39	0.37	3.28	4.14	3.65
LiGeTe <sub>2</sub>	38.31	37.98	38.14	12.13	6.34	9.24	32.92	18.03	25.64	0.36	0.42	0.39	3.16	5.99	4.13
LiSnTe <sub>2</sub>	34.48	33.76	34.12	13.10	11.25	12.17	34.88	30.38	32.64	0.33	0.35	0.34	2.63	3.00	2.81
LiPbTe <sub>2</sub>	32.98	32.82	32.90	3.19	-178.48	-87.64	9.28	658.76	-2348.38	0.45	-2.85	12.40	10.33	-0.18	-0.38

Table S XXV: Elastic moduli and ratios for lithium-intercalated TMDC tellurides.

MgMX <sub>2</sub>	Bulk Modulus (GPa)			Shear Modulus (GPa)			Young's Modulus (GPa)			Poisson Ratio			Pugh Ratio		
	V	R	H	V	R	H	V	R	H	V	R	H	V	R	H
MgScS <sub>2</sub>	91.99	91.13	91.56	59.48	58.35	58.91	146.79	144.25	145.52	0.23	0.24	0.24	1.55	1.56	1.55
MgYS <sub>2</sub>	85.02	84.14	84.58	52.88	50.02	51.45	131.41	125.24	128.33	0.24	0.25	0.25	1.61	1.68	1.64
MgTiS <sub>2</sub>	103.27	101.67	102.47	63.89	61.35	62.62	158.90	153.22	156.06	0.24	0.25	0.25	1.62	1.66	1.64
MgZrS <sub>2</sub>	107.15	106.16	106.66	64.74	61.88	63.31	161.66	155.44	158.56	0.25	0.26	0.25	1.66	1.72	1.68
MgHfS <sub>2</sub>	113.77	113.27	113.52	65.74	62.56	64.15	165.36	158.51	161.94	0.26	0.27	0.26	1.73	1.81	1.77
MgVS <sub>2</sub>	93.26	93.23	93.24	50.95	48.40	49.68	129.31	123.78	126.55	0.27	0.28	0.27	1.83	1.93	1.88
MgNbS <sub>2</sub>	119.88	117.01	118.45	68.00	63.50	65.75	171.56	161.31	166.45	0.26	0.27	0.27	1.76	1.84	1.80
MgTaS <sub>2</sub>	126.00	123.94	124.97	62.26	56.42	59.34	160.37	146.95	153.69	0.29	0.30	0.30	2.02	2.20	2.11
MgCrS <sub>2</sub>	69.22	-30.99	19.11	47.56	-58.25	-5.35	116.09	-107.44	-17.69	0.22	-0.08	0.65	1.46	0.53	-3.58
MgMoS <sub>2</sub>	121.69	111.69	116.69	56.83	46.83	51.83	147.53	123.27	135.45	0.30	0.32	0.31	2.14	2.38	2.25
MgWS <sub>2</sub>	119.98	115.81	117.90	51.58	48.03	49.81	135.34	126.60	130.97	0.31	0.32	0.31	2.33	2.41	2.37
MgMnS <sub>2</sub>	-979.09	461.22	-258.94	-55.57	28.55	-13.51	-163.60	83.91	-39.84	0.47	0.47	0.47	17.62	16.16	19.17
MgReS <sub>2</sub>	115.11	113.62	114.36	-144.37	102.67	-20.85	-744.29	236.71	-66.61	1.58	0.15	0.60	-0.80	1.11	-5.48
MgFeS <sub>2</sub>	91.16	90.61	90.89	44.86	43.94	44.40	115.63	113.49	114.56	0.29	0.29	0.29	2.03	2.06	2.05
MgRuS <sub>2</sub>	121.70	121.35	121.53	61.38	57.36	59.37	157.65	148.65	153.17	0.28	0.30	0.29	1.98	2.12	2.05
MgOsS <sub>2</sub>	125.87	125.73	125.80	66.64	60.63	63.64	169.94	156.70	163.36	0.27	0.29	0.28	1.89	2.07	1.98
MgCoS <sub>2</sub>	103.99	103.99	103.99	38.68	27.33	33.01	103.25	75.40	89.55	0.33	0.38	0.36	2.69	3.81	3.15
MgRhS <sub>2</sub>	107.50	107.35	107.43	26.97	23.77	25.37	74.66	66.41	70.55	0.38	0.40	0.39	3.99	4.52	4.23
MgIrS <sub>2</sub>	111.36	111.36	111.36	27.18	15.59	21.38	75.41	44.67	60.29	0.39	0.43	0.41	4.10	7.14	5.21
MgNiS <sub>2</sub>	92.55	92.55	92.55	46.50	45.76	46.13	119.49	117.85	118.67	0.28	0.29	0.29	1.99	2.02	2.01
MgPdS <sub>2</sub>	95.95	95.68	95.81	3.33	102.97	53.15	9.88	227.35	134.57	0.48	0.10	0.27	28.80	0.93	1.80
MgPtS <sub>2</sub>	100.00	99.50	99.75	-14.05	56.11	21.03	-44.23	141.70	58.94	0.57	0.26	0.40	-7.12	1.77	4.74
MgCuS <sub>2</sub>	88.05	87.75	87.90	17.47	-114.24	-48.39	49.16	-605.50	-177.78	0.41	1.65	0.84	5.04	-0.77	-1.82
MgAgS <sub>2</sub>	78.43	78.39	78.41	-4.01	63.91	29.95	-12.25	150.76	79.70	0.53	0.18	0.33	-19.54	1.23	2.62
MgAuS <sub>2</sub>	87.76	87.67	87.71	-30.73	48.85	9.06	-104.38	123.59	26.27	0.70	0.27	0.45	-2.86	1.79	9.68
MgGeS <sub>2</sub>	72.49	72.31	72.40	44.87	41.75	43.31	111.58	105.03	108.33	0.24	0.26	0.25	1.62	1.73	1.67
MgSnS <sub>2</sub>	66.50	65.41	65.96	36.72	31.24	33.98	93.03	80.85	87.00	0.27	0.29	0.28	1.81	2.09	1.94
MgPbS <sub>2</sub>	65.54	64.54	65.04	37.59	31.25	34.42	94.67	80.71	87.77	0.26	0.29	0.28	1.74	2.07	1.90

Table S XXVI: Elastic moduli and ratios for magnesium-intercalated TMDC sulfides.

MgMX <sub>2</sub>	Bulk Modulus (GPa)			Shear Modulus (GPa)			Young's Modulus (GPa)			Poisson Ratio			Pugh Ratio		
	V	R	H	V	R	H	V	R	H	V	R	H	V	R	H
MgSeSe <sub>2</sub>	75.55	75.01	75.28	46.31	45.18	45.75	115.36	112.88	114.12	0.25	0.25	0.25	1.63	1.66	1.65
MgYSe <sub>2</sub>	70.88	70.47	70.68	42.35	39.63	40.99	105.96	100.12	103.05	0.25	0.26	0.26	1.67	1.78	1.72
MgTiSe <sub>2</sub>	81.16	79.66	80.41	44.48	40.17	42.32	112.82	103.16	108.02	0.27	0.28	0.28	1.82	1.98	1.90
MgZnSe <sub>2</sub>	87.22	86.04	86.63	48.19	44.25	46.22	122.09	113.32	117.72	0.27	0.28	0.27	1.81	1.94	1.87
MgHS <sub>2</sub>	89.18	88.85	89.02	47.63	43.86	45.75	121.29	112.99	117.17	0.27	0.29	0.28	1.87	2.03	1.95
MgVSe <sub>2</sub>	78.29	78.25	78.27	40.99	38.94	39.96	104.69	100.20	102.45	0.28	0.29	0.28	1.91	2.01	1.96
MgNbSe <sub>2</sub>	95.45	89.62	92.54	44.90	38.33	41.61	116.44	100.64	108.57	0.30	0.31	0.30	2.13	2.34	2.22
MgTaSe <sub>2</sub>	94.03	93.60	93.81	37.46	33.47	35.47	99.21	89.72	94.49	0.32	0.34	0.33	2.51	2.80	2.65
MgCrSe <sub>2</sub>	1405.56	1857.10	1676.33	-153.45	-160.44	-156.94	-476.65	-495.60	-486.00	0.55	0.54	0.55	-9.75	-11.57	-10.68
MgMoSe <sub>2</sub>	90.34	90.25	90.29	43.20	37.41	40.31	111.78	98.61	105.26	0.29	0.32	0.31	2.09	2.41	2.24
MgWSe <sub>2</sub>	89.52	88.86	89.19	41.69	33.18	37.44	108.27	88.53	98.53	0.30	0.33	0.32	2.15	2.68	2.38
MgMnSe <sub>2</sub>	193.97	30.93	112.45	58.28	29.92	44.10	158.93	67.87	117.00	0.36	0.13	0.33	3.33	1.03	2.55
MgReSe <sub>2</sub>	98.18	98.02	98.10	26.76	-55.45	-14.34	73.60	-205.00	-45.23	0.38	0.85	0.58	3.67	-1.77	-6.84
MgFeSe <sub>2</sub>	97.30	96.23	96.77	54.45	53.87	54.16	137.67	136.20	136.94	0.26	0.26	0.26	1.79	1.79	1.79
MgRuSe <sub>2</sub>	103.13	101.69	102.41	52.08	50.05	51.07	133.73	129.00	131.36	0.28	0.29	0.29	1.98	2.03	2.01
MgOsSe <sub>2</sub>	106.99	106.24	106.62	57.83	55.63	56.73	147.01	142.09	144.56	0.27	0.28	0.27	1.85	1.92	1.88
MgCoSe <sub>2</sub>	87.46	87.20	87.33	31.95	25.97	28.96	85.44	70.87	78.23	0.34	0.36	0.35	2.74	3.36	3.02
MgRhSe <sub>2</sub>	93.62	92.89	93.25	28.67	28.02	28.35	78.05	76.38	77.21	0.36	0.36	0.36	3.27	3.33	3.29
MgIrSe <sub>2</sub>	97.25	96.86	97.05	29.63	25.75	27.69	80.70	70.95	75.85	0.36	0.38	0.37	3.28	3.76	3.51
MgNiSe <sub>2</sub>	78.47	78.44	78.45	31.51	29.41	30.46	83.37	78.43	80.91	0.32	0.33	0.33	2.49	2.67	2.58
MgPdSe <sub>2</sub>	81.12	80.76	80.94	9.82	-35.93	-13.06	28.31	-126.56	-41.40	0.44	0.76	0.59	8.26	-2.25	-6.20
MgPtSe <sub>2</sub>	84.35	84.35	84.35	5.95	163.84	84.90	17.43	298.35	190.71	0.47	-0.09	0.12	14.18	0.51	0.99
MgCuSe <sub>2</sub>	75.49	75.35	75.42	7.55	215.10	111.32	21.91	330.67	223.84	0.45	-0.23	0.01	10.00	0.35	0.68
MgAgSe <sub>2</sub>	68.04	68.04	68.04	3.92	98.79	51.35	11.54	199.71	123.09	0.47	0.01	0.20	17.36	0.69	1.32
MgAuSe <sub>2</sub>	74.48	74.46	74.47	-9.30	37.81	14.26	-29.11	97.01	40.20	0.57	0.28	0.41	-8.02	1.97	5.22
MgGeSe <sub>2</sub>	63.05	62.98	63.02	38.42	35.83	37.12	95.79	90.36	93.09	0.25	0.26	0.25	1.64	1.76	1.70
MgSnSe <sub>2</sub>	57.55	57.10	57.32	31.65	27.29	29.47	80.23	70.62	75.47	0.27	0.29	0.28	1.83	2.09	1.95
MgPbSe <sub>2</sub>	56.35	55.77	56.06	31.67	26.50	29.08	80.02	68.63	74.39	0.26	0.29	0.28	1.78	2.10	1.93

Table S XXVII: Elastic moduli and ratios for magnesium-intercalated TMDC selenides.

MgMX <sub>2</sub>	Bulk Modulus (GPa)			Shear Modulus (GPa)			Young's Modulus (GPa)			Poisson Ratio			Pugh Ratio		
	V	R	H	V	R	H	V	R	H	V	R	H	V	R	H
MgScTe <sub>2</sub>	57.74	57.64	57.69	32.50	30.72	31.61	82.10	78.26	80.19	0.26	0.27	0.27	1.78	1.88	1.83
MgYTe <sub>2</sub>	54.01	53.51	53.76	30.53	27.24	28.89	77.07	69.87	73.50	0.26	0.28	0.27	1.77	1.96	1.86
MgTiTe <sub>2</sub>	40.09	39.66	39.88	27.91	22.60	25.26	67.97	56.99	62.57	0.22	0.26	0.24	1.44	1.75	1.58
MgZrTe <sub>2</sub>	65.78	62.46	64.12	27.50	14.85	21.17	72.41	41.27	57.22	0.32	0.39	0.35	2.39	4.21	3.03
MgHTe <sub>2</sub>	64.37	63.36	63.87	28.49	18.01	23.25	74.49	49.36	62.20	0.31	0.37	0.34	2.26	3.52	2.75
MgVTe <sub>2</sub>	61.79	60.98	61.39	31.70	29.88	30.79	81.22	77.04	79.14	0.28	0.29	0.29	1.95	2.04	1.99
MgNbTe <sub>2</sub>	71.63	70.50	71.07	30.45	19.64	25.04	80.01	53.92	67.23	0.31	0.37	0.34	2.35	3.59	2.84
MgTaTe <sub>2</sub>	69.85	69.56	69.70	-11.06	74.89	31.92	-35.02	165.33	83.07	0.58	0.10	0.30	-6.32	0.93	2.18
MgCrTe <sub>2</sub>	59.27	59.15	59.21	21.98	21.33	21.66	58.69	57.12	57.91	0.33	0.34	0.34	2.70	2.77	2.73
MgMoTe <sub>2</sub>	72.39	71.63	72.01	37.62	33.55	35.59	96.20	87.06	91.66	0.28	0.30	0.29	1.92	2.13	2.02
MgWTe <sub>2</sub>	75.98	75.77	75.88	38.70	34.66	36.68	99.24	90.23	94.77	0.28	0.30	0.29	1.96	2.19	2.07
MgMnTe <sub>2</sub>	60.11	-29.84	15.13	27.32	-42.72	-7.70	71.17	-86.75	-27.82	0.30	0.02	0.81	2.20	0.70	-1.97
MgReTe <sub>2</sub>	83.73	83.28	83.50	41.55	39.91	40.73	106.95	103.23	105.10	0.29	0.29	0.29	2.02	2.09	2.05
MgFeTe <sub>2</sub>	77.51	74.25	75.88	44.43	41.23	42.83	111.90	104.36	108.14	0.26	0.27	0.26	1.74	1.80	1.77
MgRuTe <sub>2</sub>	83.85	80.29	82.07	45.64	44.21	44.93	115.89	112.07	113.98	0.27	0.27	0.27	1.84	1.82	1.83
MgOsTe <sub>2</sub>	91.13	88.29	89.71	54.47	53.70	54.08	136.27	133.93	135.10	0.25	0.25	0.25	1.67	1.64	1.66
MgCoTe <sub>2</sub>	70.03	68.53	69.28	29.09	24.12	26.61	76.66	64.76	70.76	0.32	0.34	0.32	2.41	2.84	2.60
MgRhTe <sub>2</sub>	75.21	72.04	73.63	26.76	23.64	25.20	71.77	63.92	67.86	0.34	0.35	0.35	2.81	3.05	2.92
MgIrTe <sub>2</sub>	81.99	79.73	80.85	27.65	18.21	22.93	74.57	50.77	62.85	0.35	0.39	0.37	2.97	4.38	3.53
MgNiTe <sub>2</sub>	67.24	66.07	66.65	17.86	9.94	13.90	49.22	28.41	39.00	0.38	0.43	0.40	3.76	6.64	4.79
MgPdTe <sub>2</sub>	66.90	64.49	65.70	15.39	10.86	13.13	42.88	30.85	36.92	0.39	0.42	0.41	4.35	5.94	5.01
MgPtTe <sub>2</sub>	72.51	70.82	71.67	15.73	0.92	8.33	44.02	2.76	24.05	0.40	0.49	0.44	4.61	76.78	8.61
MgCuTe <sub>2</sub>	58.84	58.60	58.72	6.45	111.39	58.92	18.66	204.56	132.45	0.45	-0.08	0.12	9.12	0.53	1.00
MgAgTe <sub>2</sub>	53.21	53.18	53.19	3.37	78.20	40.78	9.89	157.43	97.44	0.47	0.01	0.19	15.80	0.68	1.30
MgAuTe <sub>2</sub>	59.70	58.09	58.90	-2.83	14.87	6.02	-8.62	41.09	17.46	0.52	0.38	0.45	-21.11	3.91	9.78
MgGeTe <sub>2</sub>	48.32	48.29	48.31	31.25	29.11	30.18	77.12	72.72	74.93	0.23	0.25	0.24	1.55	1.66	1.60
MgSnTe <sub>2</sub>	46.19	46.04	46.12	26.46	23.10	24.78	66.64	59.36	63.04	0.26	0.29	0.27	1.75	1.99	1.86
MgPbTe <sub>2</sub>	45.03	44.74	44.89	25.40	21.28	23.34	64.14	55.10	59.67	0.26	0.29	0.28	1.77	2.10	1.92

Table S XXVIII: Elastic moduli and ratios for magnesium-intercalated TMDC tellurides.

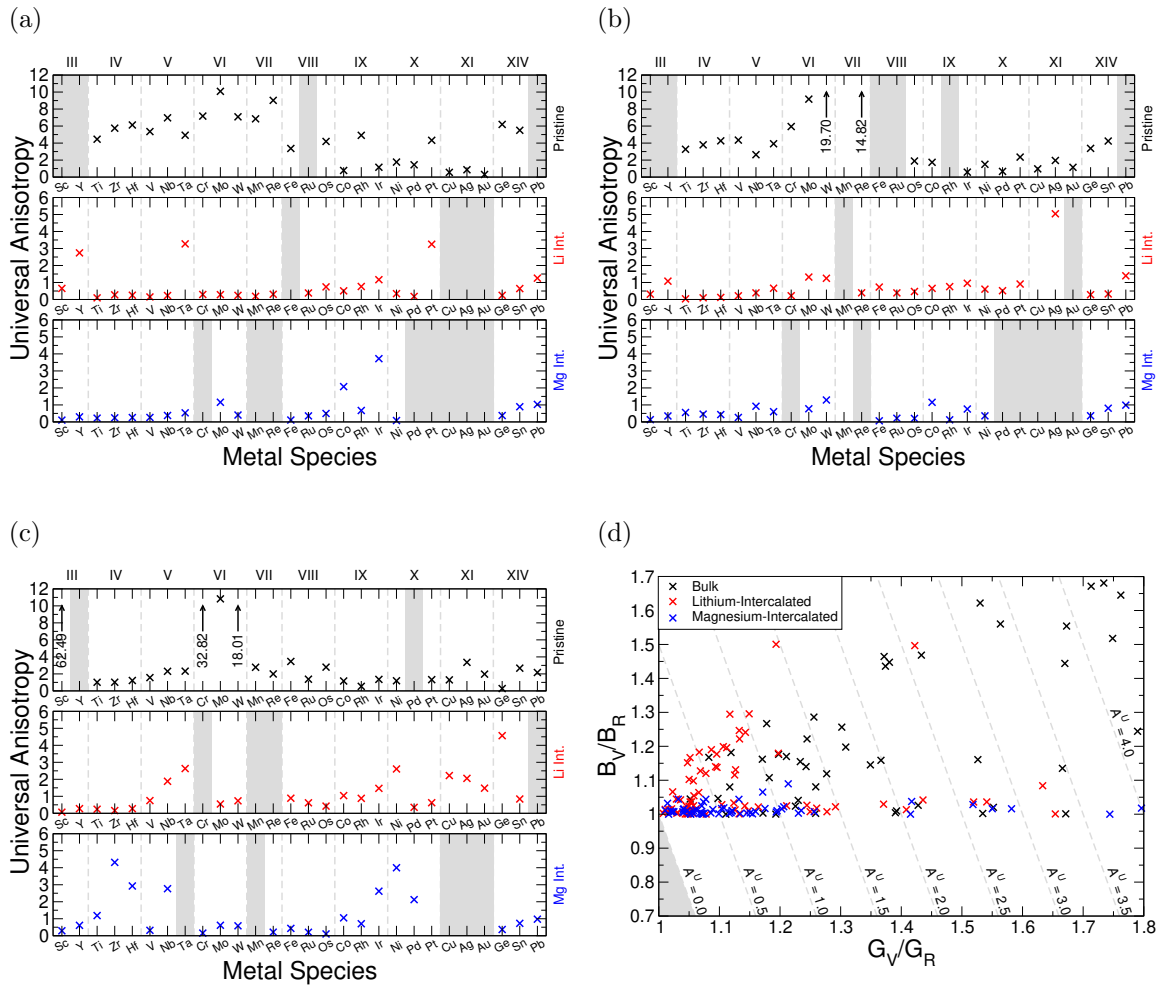


Figure S6: Universal anisotropy values for the sulfide (S6a), selenide (S6b), and telluride (S6c) materials, and data for the pristine bulk, lithium-intercalated, and magnesium-intercalated structures is presented in black, red, and blue, respectively. Arrows with labels indicate values that lie outside of the plotted range. Materials which are not elastically stable are indicated with shaded regions. S6d shows the elastic anisotropy diagram, with data for all materials included.

## E. Material Anisotropy

### 1. Universal Anisotropy and Elastic Constants

The universal anisotropy  $A^U$  is presented in Figure S6, and the elastic constants  $c_{11}$  and  $c_{33}$  are shown in Figure S7 for the sulfide, selenide, and telluride materials.

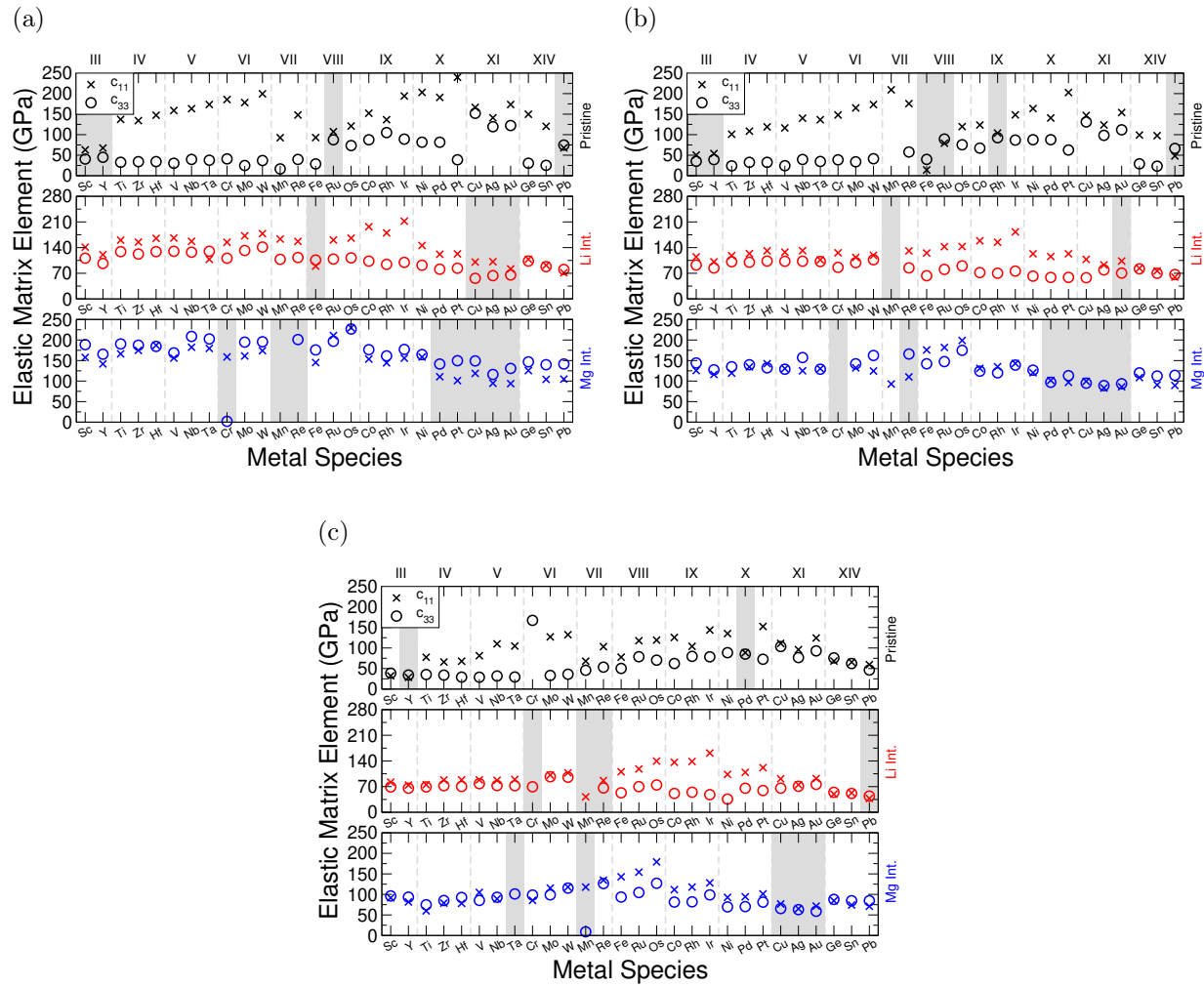


Figure S 7: Elements of the elastic matrix,  $c_{11}$  and  $c_{33}$ , for the sulfide (S7a), selenide (S7b), telluride (S7c) TMDC materials. Data for the pristine bulk, lithium-intercalated, and magnesium-intercalated structures is presented in black, red, and blue, respectively. Materials which are not elastically stable are indicated with shaded regions. Numerical values are presented in Table SIX-Table SXVII.

M	$A^U$		
	Sulfides	Selenides	Tellurides
Sc	-4.73	-4.75	62.49
Y	-4.70	-4.78	-4.81
Ti	4.46	3.27	1.02
Zr	5.75	3.79	1.02
Hf	6.13	4.26	1.22
V	5.35	4.35	1.57
Nb	6.97	2.63	2.31
Ta	4.92	3.92	2.32
Cr	7.18	5.94	32.82
Mo	10.09	9.17	10.83
W	7.09	19.70	18.01
Mn	6.85	-2.87	2.78
Re	9.02	14.82	1.99
Fe	3.36	-7.38	3.46
Ru	-63.42	-60.46	1.38
Os	4.19	1.89	2.79
Co	0.78	1.74	1.16
Rh	4.91	-12.54	0.53
Ir	1.16	0.58	1.35
Ni	1.77	1.50	1.19
Pd	1.44	0.67	-5.93
Pt	4.33	2.35	1.32
Cu	0.55	0.97	1.30
Ag	0.86	1.96	3.36
Au	0.30	1.15	1.97
Ge	6.19	3.38	0.28
Sn	5.50	4.24	2.67
Pb	-5.58	-7.47	2.17

Table S XXIX: Values of universal anisotropy index  $A^U$  for pristine TMDCs.

M	$A^U$		
	Sulfides	Selenides	Tellurides
Sc	0.65	0.31	0.07
Y	2.74	1.08	0.28
Ti	0.10	0.04	0.24
Zr	0.27	0.10	0.16
Hf	0.25	0.12	0.27
V	0.15	0.22	0.75
Nb	0.23	0.39	1.88
Ta	3.27	0.66	2.63
Cr	0.29	0.22	-6.45
Mo	0.29	1.32	0.55
W	0.24	1.25	0.73
Mn	0.19	-13.73	9.50
Re	0.31	0.39	-9.50
Fe	-5.03	0.73	0.89
Ru	0.38	0.39	0.62
Os	0.74	0.47	0.42
Co	0.51	0.66	1.04
Rh	0.76	0.76	0.88
Ir	1.17	0.96	1.47
Ni	0.34	0.61	2.61
Pd	0.18	0.52	0.35
Pt	3.25	0.91	0.62
Cu	-7.20	6.58	2.22
Ag	-5.48	5.04	2.06
Au	-7.02	-6.95	1.48
Ge	0.25	0.28	4.57
Sn	0.64	0.33	0.84
Pb	1.26	1.39	-5.08

Table S XXX: Values of universal anisotropy index  $A^U$  for lithium-intercalated TMDCs.

M	$A^U$		
	Sulfides	Selenides	Tellurides
Sc	0.11	0.13	0.29
Y	0.30	0.35	0.61
Ti	0.22	0.56	1.19
Zr	0.24	0.46	4.32
Hf	0.26	0.43	2.93
V	0.26	0.26	0.32
Nb	0.38	0.92	2.77
Ta	0.53	0.60	-5.73
Cr	-12.32	-0.41	0.16
Mo	1.16	0.77	0.62
W	0.41	1.29	0.58
Mn	-17.85	10.01	-11.21
Re	-12.02	-7.41	0.21
Fe	0.11	0.06	0.43
Ru	0.35	0.22	0.21
Os	0.50	0.21	0.10
Co	2.08	1.15	1.05
Rh	0.67	0.12	0.70
Ir	3.72	0.76	2.62
Ni	0.08	0.36	4.00
Pd	-4.84	-6.36	2.12
Pt	-6.25	-4.82	80.30
Cu	-5.76	-4.82	-4.71
Ag	-5.31	-4.80	-4.78
Au	-8.14	-6.23	-5.92
Ge	0.38	0.36	0.37
Sn	0.89	0.81	0.73
Pb	1.03	0.99	0.97

Table S XXXI: Values of universal anisotropy index  $A^U$  for magnesium-intercalated TMDCs.

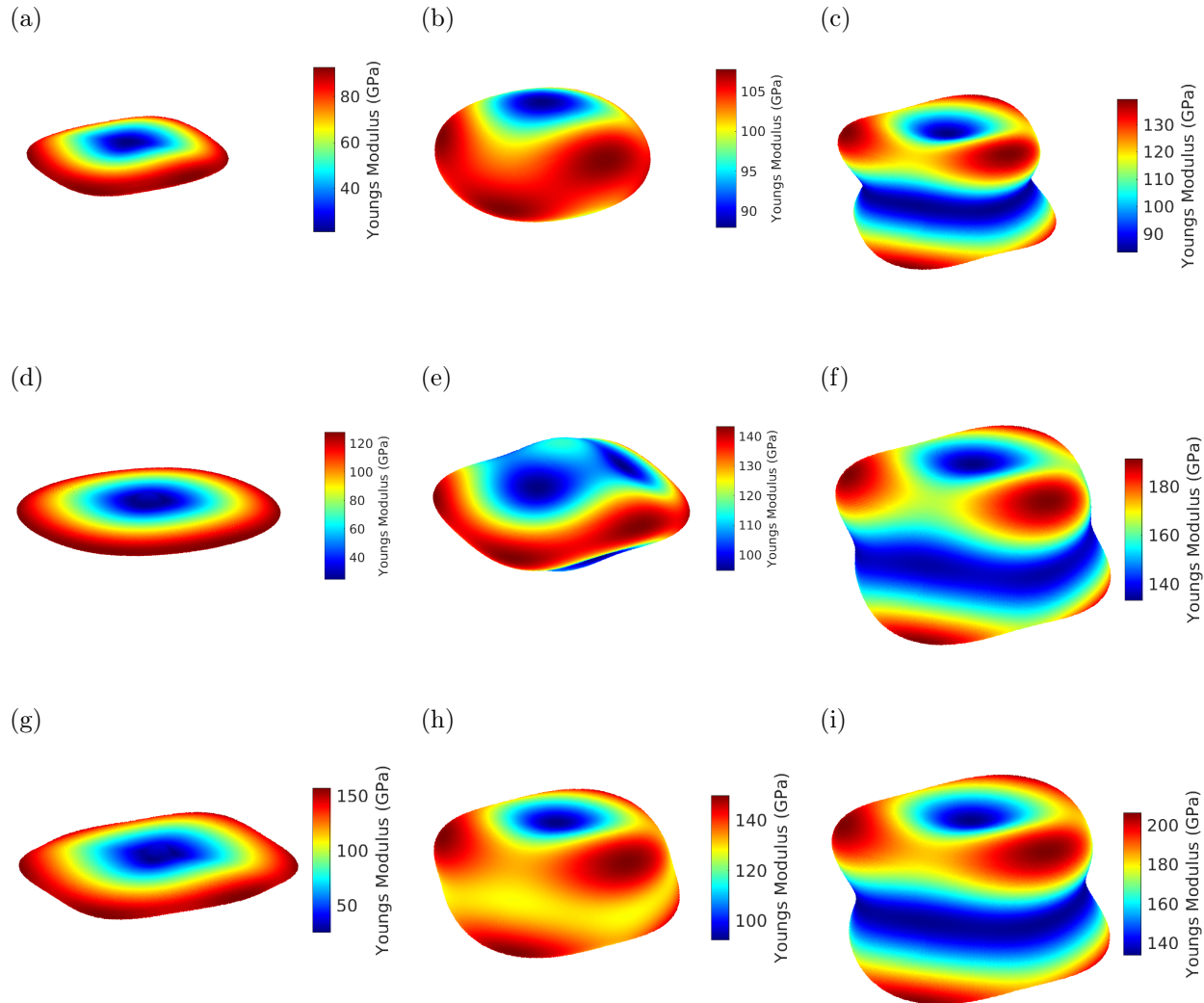


Figure S 8: Three-dimensional heat maps showing the angular-dependent Young's modulus for  $\text{TiSe}_2$  (S8a),  $\text{LiTiSe}_2$  (S8b),  $\text{MgTiSe}_2$  (S8c),  $\text{ZrS}_2$  (S8d),  $\text{LiZrS}_2$  (S8e),  $\text{MgZrS}_2$  (S8f),  $\text{NbS}_2$  (S8g),  $\text{LiNbS}_2$  (S8h), and  $\text{MgNbS}_2$  (S8i).

## 2. Anisotropic Young's Modulus

In the main article, we presented the angular dependence of the Young's modulus for  $\text{TiS}_2$ , showing how this changed with lithium and magnesium intercalation. We include here similar graphics for several other TMDC materials. In Figure S8 we show the anisotropic Young's modulus for  $\text{TiSe}_2$ ,  $\text{ZrS}_2$ , and  $\text{NbS}_2$ , in their pristine and intercalated forms, and we show in Figure S9 the anisotropic Young's modulus for  $\text{MoS}_2$ ,  $\text{WS}_2$ , and  $\text{SnS}_2$ , in their pristine and intercalated forms.

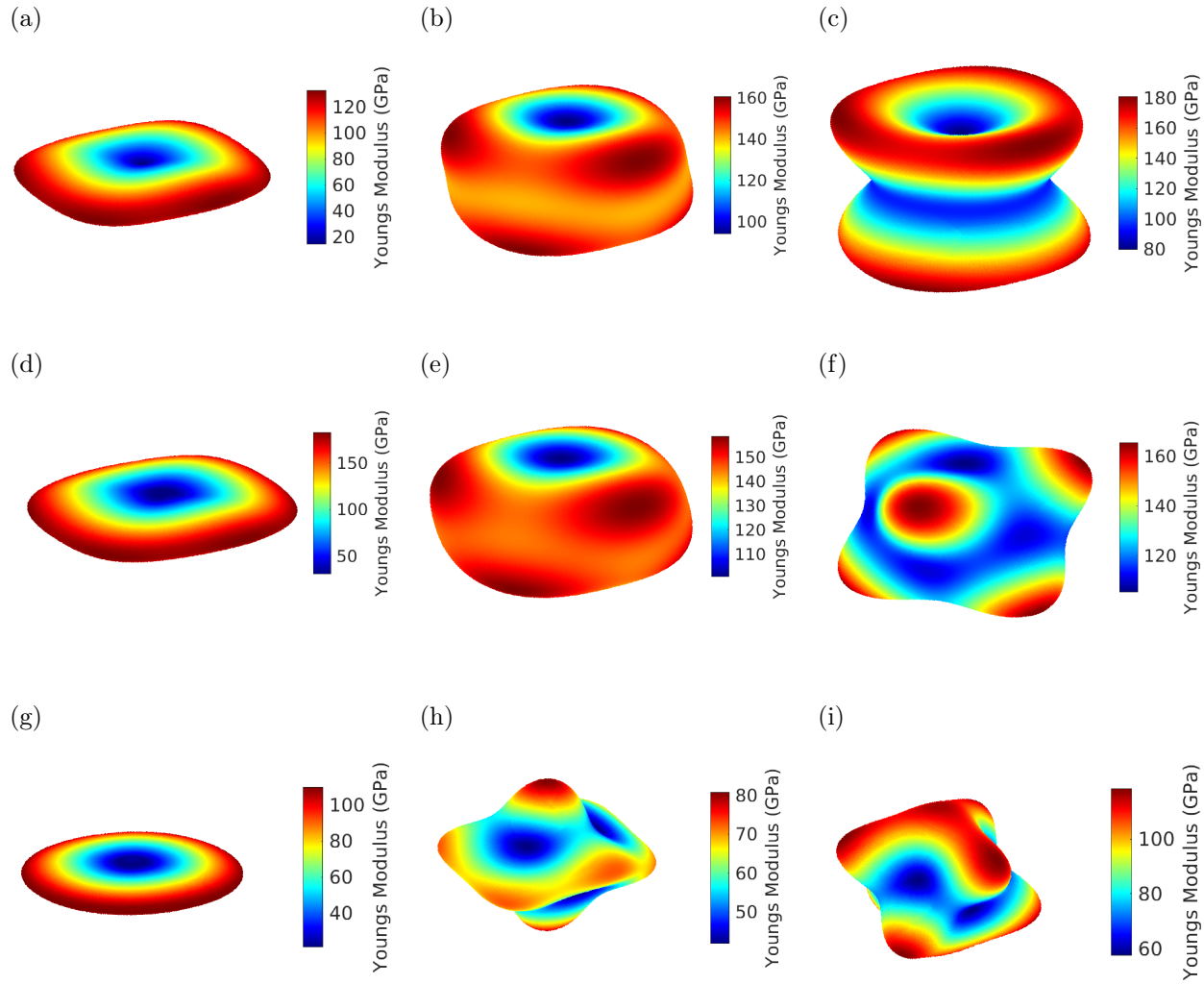


Figure S 9: Three-dimensional heat maps showing the angular-dependent Young's modulus for MoS<sub>2</sub> (S9a), LiMoS<sub>2</sub> (S9b), MgMoS<sub>2</sub> (S9c), WS<sub>2</sub> (S9d), LiWS<sub>2</sub> (S9e), MgWS<sub>2</sub> (S9f), SnS<sub>2</sub> (S9g), LiSnS<sub>2</sub> (S9h), and MgSnS<sub>2</sub> (S9i).

In each of these, we see that the out-of-plane Young's modulus for the pristine structures is significantly smaller (with values below 50 GPa) than the in-plane Young's modulus (with values exceeding 100 GPa). Due to the strong in-plane covalent bonding and weak out-of-plane vdW bonding, this is to be expected. With the introduction of lithium, there is an increase in the in-plane Young's modulus, but a more dramatic increase in the out-of-plane component. This indicates the strengthened bonding between consecutive TMDC layers, facilitated by the lithium ion. We see a similar effect with magnesium intercalation, but

high Young's modulus values are achieved due to the larger charge transfer.

---

\* cjp225@exeter.ac.uk

† S.P.Hepplestone@exeter.ac.uk

- <sup>1</sup> P. E. Blöchl, Physical Review B **50**, 17953 (1994).
- <sup>2</sup> J. P. Perdew, K. Burke, and M. Ernzerhof, Physical Review Letters **77**, 3865 (1996).
- <sup>3</sup> H. J. Monkhorst and J. D. Pack, Physical Review B **13**, 5188 (1976).
- <sup>4</sup> S. Grimme, J. Antony, S. Ehrlich, and H. Krieg, The Journal of Chemical Physics **132**, 154104 (2010).
- <sup>5</sup> F. Zhou, M. Cococcioni, C. A. Marianetti, D. Morgan, and G. Ceder, Physical Review B - Condensed Matter and Materials Physics **70**, 1 (2004), arXiv:0406382 [cond-mat].
- <sup>6</sup> V. L. Chevrier, S. P. Ong, R. Armiento, M. K. Chan, and G. Ceder, Physical Review B - Condensed Matter and Materials Physics **82**, 1 (2010).
- <sup>7</sup> M. Barhoumi and N. Sfina, ACS Omega **7**, 15338 (2022).
- <sup>8</sup> M. Barhoumi, Results in Physics **45**, 106251 (2023).
- <sup>9</sup> J. Kaczkowski, Materials Chemistry and Physics **177**, 405 (2016).
- <sup>10</sup> G. Li, Q. An, S. I. Morozov, B. Duan, P. Zhai, Q. Zhang, W. A. Goddard III, and G. J. Snyder, Journal of Materials Chemistry A **6**, 11743 (2018).
- <sup>11</sup> T. Maxisch and G. Ceder, Physical Review B **73**, 174112 (2006).
- <sup>12</sup> S. A. Yamusa, A. Shaari, N. A. M. Alsaif, I. M. Alsalamah, I. Isah, and N. Rekik, ACS Omega **7**, 45719 (2022).
- <sup>13</sup> H. Peelaers and C. G. Van de Walle, The Journal of Physical Chemistry C **118**, 12073 (2014).
- <sup>14</sup> J.-n. Yuan, Y. Cheng, X.-q. Zhang, X.-r. Chen, and L.-c. Cai, Zeitschrift für Naturforschung A **70**, 529 (2015).
- <sup>15</sup> L. Liu, J. Cao, W. Guo, and C. Wang, Chinese Physics B **31**, 016105 (2022).
- <sup>16</sup> J. Bera, A. Betal, and S. Sahu, Journal of Alloys and Compounds **872**, 159704 (2021).
- <sup>17</sup> M. Goyal and M. Sinha, Journal of Physics and Chemistry of Solids **153**, 110024 (2021).
- <sup>18</sup> Y. Qi, L. G. Hector, C. James, and K. J. Kim, Journal of The Electrochemical Society **161**, F3010 (2014).
- <sup>19</sup> A. Jain, S. P. Ong, G. Hautier, W. Chen, W. D. Richards, S. Dacek, S. Cholia, D. Gunter,

- D. Skinner, G. Ceder, and K. A. Persson, *APL Materials* **1**, 011002 (2013).
- <sup>20</sup> M. de Jong, W. Chen, T. Angsten, A. Jain, R. Notestine, A. Gamst, M. Sluiter, C. Krishna Ande, S. van der Zwaag, J. J. Plata, C. Toher, S. Curtarolo, G. Ceder, K. A. Persson, and M. Asta, *Scientific Data* **2**, 150009 (2015).
- <sup>21</sup> Y. Qi, H. Guo, L. G. Hector, and A. Timmons, *Journal of The Electrochemical Society* **157**, A558 (2010).
- <sup>22</sup> S. Shang, Y. Wang, P. Guan, W. Y. Wang, H. Fang, T. Anderson, and Z.-K. Liu, *Journal of Materials Chemistry A* **3**, 8002 (2015).
- <sup>23</sup> R. W. McKinney, P. Gorai, S. Manna, E. Toberer, and V. Stevanović, *Journal of Materials Chemistry A* **6**, 15828 (2018), arXiv:1805.10489.
- <sup>24</sup> M. Woodcox, R. Shepard, and M. Smeu, *Journal of Power Sources* **516**, 230620 (2021).
- <sup>25</sup> B. Mortazavi, M. Shahrokhi, X. Zhuang, T. Rabczuk, and A. V. Shapeev, *Journal of Materials Chemistry C* **10**, 329 (2022).
- <sup>26</sup> K. R. Kganyago and P. E. Nguope, *Physical Review B* **68**, 205111 (2003).
- <sup>27</sup> K. H. Michel and B. Verberck, *physica status solidi (b)* **245**, 2177 (2008).
- <sup>28</sup> A. P. P. Nicholson and D. J. Bacon, *Journal of Physics C: Solid State Physics* **10**, 2295 (1977).
- <sup>29</sup> L. Lang, S. Doyen-Lang, A. Charlier, and M. F. Charlier, *Physical Review B* **49**, 5672 (1994).
- <sup>30</sup> R. Al-Jishi and G. Dresselhaus, *Physical Review B* **26**, 4514 (1982).
- <sup>31</sup> O. L. Blakslee, D. G. Proctor, E. J. Seldin, G. B. Spence, and T. Weng, *Journal of Applied Physics* **41**, 3373 (1970).
- <sup>32</sup> E. J. Seldin and C. W. Nezbeda, *Journal of Applied Physics* **41**, 3389 (1970).
- <sup>33</sup> H. Zabel, W. A. Kamitakahara, and R. M. Nicklow, *Physical Review B* **26**, 5919 (1982).
- <sup>34</sup> H. Zabel and A. Magerl, *Physical Review B* **25**, 2463 (1982).
- <sup>35</sup> M. Grimsditch, *Journal of Physics C: Solid State Physics* **16**, L143 (1983).
- <sup>36</sup> T. M. Project, “Materials Data on LiCoO<sub>2</sub> (SG:166) by Materials Project,” (2014).
- <sup>37</sup> S. Yamakawa, N. Nagasako, H. Yamasaki, T. Koyama, and R. Asahi, *Solid State Ionics* **319**, 209 (2018).
- <sup>38</sup> F. X. Hart and J. B. Bates, *Journal of Applied Physics* **83**, 7560 (1998).
- <sup>39</sup> X. Wang, I. Loa, K. Kunc, K. Syassen, and M. Amboage, *Physical Review B* **72**, 224102 (2005).
- <sup>40</sup> E. J. Cheng, N. J. Taylor, J. Wolfenstine, and J. Sakamoto, *Journal of Asian Ceramic Societies* **5**, 113 (2017).

- <sup>41</sup> M. Qu, W. H. Woodford, J. M. Maloney, W. C. Carter, Y.-M. Chiang, and K. J. Van Vliet, Advanced Energy Materials **2**, 940 (2012).
- <sup>42</sup> C. J. Price, E. A. D. Baker, and S. P. Hepplestone, Journal of Materials Chemistry A **11**, 12354 (2023).
- <sup>43</sup> M. Wang, S. Xu, and J. J. Cha, Advanced Energy and Sustainability Research **2**, 2100027 (2021).
- <sup>44</sup> Y. Wu, J. Wang, Y. Li, J. Zhou, B. Y. Wang, A. Yang, L.-W. Wang, H. Y. Hwang, and Y. Cui, Nature Communications **13**, 3008 (2022).
- <sup>45</sup> T. M. Project, “Materials Data on TiS<sub>2</sub> by Materials Project,” (2020).
- <sup>46</sup> T. M. Project, “Materials Data on LiTiS<sub>2</sub> by Materials Project,” (2020).
- <sup>47</sup> T. M. Project, “Materials Data on TiSe<sub>2</sub> by Materials Project,” (2017).
- <sup>48</sup> T. M. Project, “Materials Data on TiTe<sub>2</sub> by Materials Project,” (2020).
- <sup>49</sup> T. M. Project, “Materials Data on LiTiTe<sub>2</sub> by Materials Project,” (2020).
- <sup>50</sup> T. M. Project, “Materials Data on ZrS<sub>2</sub> by Materials Project,” (2020).
- <sup>51</sup> T. M. Project, “Materials Data on ZrSe<sub>2</sub> by Materials Project,” (2020).
- <sup>52</sup> T. M. Project, “Materials Data on ZrTe<sub>2</sub> by Materials Project,” (2020).
- <sup>53</sup> T. M. Project, “Materials Data on HfTe<sub>2</sub> by Materials Project,” (2020).
- <sup>54</sup> T. M. Project, “Materials Data on LiVS<sub>2</sub> by Materials Project,” (2020).
- <sup>55</sup> T. M. Project, “Materials Data on VSe<sub>2</sub> by Materials Project,” (2020).
- <sup>56</sup> T. M. Project, “Materials Data on NbS<sub>2</sub> by Materials Project,” (2020).
- <sup>57</sup> T. M. Project, “Materials Data on NbSe<sub>2</sub> by Materials Project,” (2020).
- <sup>58</sup> T. M. Project, “Materials Data on CrS<sub>2</sub> by Materials Project,” (2020).
- <sup>59</sup> T. M. Project, “Materials Data on CrTe<sub>2</sub> by Materials Project,” (2020).
- <sup>60</sup> T. M. Project, “Materials Data on SnS<sub>2</sub> by Materials Project,” (2020).
- <sup>61</sup> T. M. Project, “Materials Data on SnSe<sub>2</sub> by Materials Project,” (2020).
- <sup>62</sup> F. Mouhat and F.-X. Coudert, Physical Review B **90**, 224104 (2014).